

## Chapter 7

# Modelling N<sub>2</sub>O production and emissions

Mathieu Spérandio<sup>1</sup>, Longqi Lang<sup>1</sup>, Fabrizio Sabba<sup>2</sup>, Robert Nerenberg<sup>2</sup>, Peter Vanrolleghem<sup>3</sup>, Carlos Domingo-Félez<sup>4</sup>, Barth F. Smets<sup>4</sup>, Haoran Duan<sup>5</sup>, Bing-Jie Ni<sup>5</sup> and Zhiguo Yuan<sup>5</sup>

<sup>1</sup>TBI, Université de Toulouse, CNRS, INRAE, INSA, Toulouse, France. E-mail: sperandio@insa-toulouse.fr

<sup>2</sup>Department of Civil and Environmental Engineering and Earth Sciences, University of Notre Dame, Notre Dame, IN 46556, USA

<sup>3</sup>Modeleau, Département de génie civil et de génie des eaux, Université Laval, 1065 av. de la Médecine, Québec, QC G1V 0A6, Canada

<sup>4</sup>Department of Environmental Engineering, Technical University of Denmark, 2800 Kongens Lyngby, Denmark

<sup>5</sup>Advanced Water Management Centre, The University of Queensland, St Lucia, QLD 4072, Australia. E-mail: z.yuan@awmc.uq.edu.au

### SUMMARY

Mathematical modelling of N<sub>2</sub>O emissions is of great importance for the understanding and reduction of the environmental impact of wastewater treatment systems. This chapter reviews the current status of the modelling of N<sub>2</sub>O emissions from wastewater treatment. The existing mathematical models describing all known microbial pathways for N<sub>2</sub>O production are reviewed and discussed. These include N<sub>2</sub>O production and consumption by heterotrophic denitrifiers, N<sub>2</sub>O production by ammonia-oxidizing bacteria (AOB) through the hydroxylamine oxidation pathway and the AOB denitrification pathway and the integration of these pathways in single-pathway N<sub>2</sub>O models. The two-pathway models are compared to single-pathway models. The calibration and validation of these models using lab-scale and full-scale experimental data is also reviewed. The mathematical modelling of N<sub>2</sub>O production, while still being enhanced by new knowledge development, has reached a maturity that facilitates the estimation of site-specific N<sub>2</sub>O emissions and the development of mitigation strategies for wastewater treatment plants taking into account the specific design and operational conditions of the plant.

**Keywords:** AOB pathways, calibration, heterotrophic denitrification, modelling, N<sub>2</sub>O

### TERMINOLOGY

Term	Definition
Mathematical model	A system of mathematical equations that describes physical and biological processes. It is a simplified representation of the real process.
Model parameters	Model parameters are model constituents (stoichiometric and kinetic) determined according to model applications. The value of a parameter for the given application is ideally constant.

© 2022 The Editors. This is an Open Access book chapter distributed under a Creative Commons Attribution Non Commercial 4.0 International License (CCBY-NC 4.0), (<https://creativecommons.org/licenses/by-nc-nd/4.0/>). The chapter is from the book *Quantification and Modelling of Fugitive Greenhouse Gas Emissions from Urban Water Systems*, Liu Ye, Jose Porro and Ingmar Nopens (Eds.).

State variables	State variables represent time-varying concentrations or other properties to be determined by a solver based on their derivatives.
Model calibration	The estimation and adjustment of model parameters to enhance the agreement between model output and experimental data.
Model validation	The comparison of model simulated output with real observations using data not used in model development. The model is validated if the simulation during the validation period lies within acceptable limits around the observations.
Kinetics	Kinetics describe the rate of chemical or biological reactions, by considering factors that influence the rate of reactions. Kinetics are associated with the fundamental mechanisms of the reaction.
Stoichiometric relationship	The quantitative relationship among the amounts of substances consumed or produced in a chemical or biological reaction.
Metabolic pathway	A series of biochemical reactions occurring within microorganisms. The reactants, products, and intermediates of an enzymatic reaction which are known as metabolites, are linked by the metabolic pathway.
Emission factor (N <sub>2</sub> O)	The N <sub>2</sub> O emission factor is defined as the ratio between N <sub>2</sub> O nitrogen emitted and the ammonium nitrogen converted.

## 7.1 INTRODUCTION

Mathematical models have been widely applied to the prediction of nitrogen removal in wastewater treatment, and are gaining increasing attention for the prediction of N<sub>2</sub>O accumulation and emission during nitrification and denitrification processes (CH2MHill, 2008; Corominas *et al.*, 2012; Guo and Vanrolleghem, 2014; Harper *et al.*, 2015; Hiatt and Grady, 2008; Mannina *et al.*, 2016; Ni *et al.*, 2011; Pocquet *et al.*, 2013). The ability to predict N<sub>2</sub>O production by modelling provides an opportunity to include N<sub>2</sub>O production as an important consideration in the design, operation and optimization of biological nitrogen removal processes (Ni *et al.*, 2011, 2013a). Furthermore, mathematical modelling should be a more appropriate method for estimating site-specific emissions of N<sub>2</sub>O than oversimplified models with fixed N<sub>2</sub>O emission factors (Corominas *et al.*, 2012; Guo and Vanrolleghem, 2014; Mampaey *et al.*, 2013; Ni *et al.*, 2011, 2013a; Pocquet *et al.*, 2013). In addition, mathematical modelling provides a method for verifying hypotheses related to the mechanisms for N<sub>2</sub>O production, and thus serves as a tool to support the development of mitigation strategies (Duan *et al.*, 2020; Ni *et al.*, 2013b; Vasilaki *et al.*, 2020; Zaborowska *et al.*, 2019).

N<sub>2</sub>O modelling has evolved rapidly in the past few years, with models based on various production pathways proposed. These models have been calibrated with data obtained from laboratory reactors and full-scale wastewater treatment plants operated under various conditions. Each of these models has its underlying assumptions and has been calibrated/validated to various degrees based on the understanding of the processes of the distinct model creators. These models displayed various predictive abilities (usually good fit with own data but failure with foreign data). Despite the obvious importance of N<sub>2</sub>O modelling, and the increasing number of publications, model comparisons and comprehensive reviews are rare (Mannina *et al.*, 2016, Spérandio *et al.*, 2016). This chapter aims to compare these models and provide guidance for their use. The existing mathematical models describing all known microbial and chemical pathways for N<sub>2</sub>O production and consumption, as well as their underlying assumptions, are reviewed, discussed and compared.

This work includes the single-pathway and two-pathway models of ammonia-oxidizing bacteria (AOB), the N<sub>2</sub>O models of heterotrophic denitrifiers, and the integrated N<sub>2</sub>O models including both AOB and heterotrophic denitrifier activities. An overview of the model evaluations using lab-scale and full-scale experimental data is also presented to provide insights into the applicability of these N<sub>2</sub>O models under various conditions.

## 7.2 N<sub>2</sub>O KINETIC MODEL STRUCTURES

N<sub>2</sub>O is produced during biological nitrogen removal in wastewater treatment, typically attributed to autotrophic AOB (Chandran *et al.*, 2011; Kampschreur *et al.*, 2009; Tallec *et al.*, 2006) and heterotrophic denitrifiers (Kampschreur *et al.*, 2009; Lu and Chandran, 2010; Pan *et al.*, 2012). There are three main microbial pathways involved in N<sub>2</sub>O formation, namely the NH<sub>2</sub>OH oxidation, nitrifier (AOB) denitrification, and heterotrophic denitrification pathways (Wunderlin *et al.*, 2012, 2013). The latter pathway is the only known microbial pathway that allows N<sub>2</sub>O consumption. Table S1 in the supplementary information (SI) lists the definitions of the all the state variables used in the models described in this chapter.

In addition N<sub>2</sub>O might be potentially produced through chemical pathways (Harper *et al.*, 2015; Schreiber *et al.*, 2009). Such processes involve hydroxylamine with different oxidants (HNO<sub>2</sub>, Fe<sup>3+</sup>, O<sub>2</sub>) or hydroxylamine disproportionation, or HNO<sub>2</sub> reduction by Fe<sup>2+</sup>. The kinetic model structure for such a chemical pathway is relatively simple, based on the first order regarding the reactants for instance, as proposed for the reaction between hydroxylamine and free nitrous acid (Harper *et al.*, 2015). Moreover the recent work of Su *et al.* (2019a) demonstrated that these chemical reactions are strongly influenced by pH and become important only at acidic pH ( $\leq 5$ ). Consequently abiotic N<sub>2</sub>O production contributes little (<3% of total N<sub>2</sub>O production) to total N<sub>2</sub>O emissions in typical nitrification reactor systems between pH 6.5 and 8. Hence, in this chapter the description will be focused on biological models.

### 7.2.1 Modelling of N<sub>2</sub>O production and consumption by Heterotrophic Denitrifiers

#### 7.2.1.1 Introduction

N<sub>2</sub>O is a known intermediate in heterotrophic denitrification (Pan *et al.*, 2012, 2013a; von Schulthess and Gujer, 1996). Heterotrophic denitrification converts the nitrate and/or nitrite generated from autotrophic nitrification to nitrogen gas (N<sub>2</sub>) and thus removes nitrogen from wastewater. It consists of four consecutive steps, which produce three obligatory intermediates, namely NO<sub>2</sub><sup>-</sup>, NO and N<sub>2</sub>O. These steps are individually catalysed by four different denitrification reductases, that is nitrate reductase (Nar), nitrite reductase (Nir), NO reductase (NOR) and N<sub>2</sub>O reductase (N<sub>2</sub>OR). N<sub>2</sub>O is produced by the sequential action of the NO<sub>3</sub><sup>-</sup>, NO<sub>2</sub><sup>-</sup> and NO reductases.

Many factors could affect the denitrification process and thus impact N<sub>2</sub>O emission, such as chemical oxygen demand (COD) to N ratios, the substrate and biomass types, pH levels and temperature, among others (Lu and Chandran, 2010; Pan *et al.*, 2012, 2013a). On the other hand, the four parallel denitrification steps could also exert influence on each other through electron competition, which could result in accumulation of various intermediates including N<sub>2</sub>O. The four denitrification steps all require electrons from carbon oxidation, and they could face competition for electrons when the electron supply rate from carbon oxidation does not meet the demand for electrons by the four steps of denitrification combined (Pan *et al.*, 2013a).

To predict denitrification intermediates accumulation, denitrification needs to be modelled as a multiple-step process (von Schulthess and Gujer, 1996). Figure 7.1 gives an overview of the major models. Four-step denitrification models have been proposed and widely applied to predict the accumulation of all denitrification intermediates including N<sub>2</sub>O (Hiatt and Grady, 2008; Kampschreur *et al.*, 2007; Ni *et al.*, 2011; Pan *et al.*, 2013b). To date, two distinct concepts have been proposed (Table 7.1), which are represented by the activated sludge model for nitrogen (ASMN) (Hiatt and Grady, 2008) and the activated sludge model with indirect coupling of electrons (ASM-ICE) (Pan *et al.*, 2013b), respectively. Table S2 in the SI lists the kinetic and stoichiometric matrices for the two models, which are fundamentally different in describing the electron allocation among different steps of heterotrophic denitrification (Table 7.1).

#### 7.2.1.2 Activated sludge model for nitrogen (ASMN)

The 'direct coupling approach', represented by ASMN (Model OHO-A in Table 7.1, Hiatt and Grady, 2008), directly couples the carbon oxidation and nitrogen reduction processes in the model. This

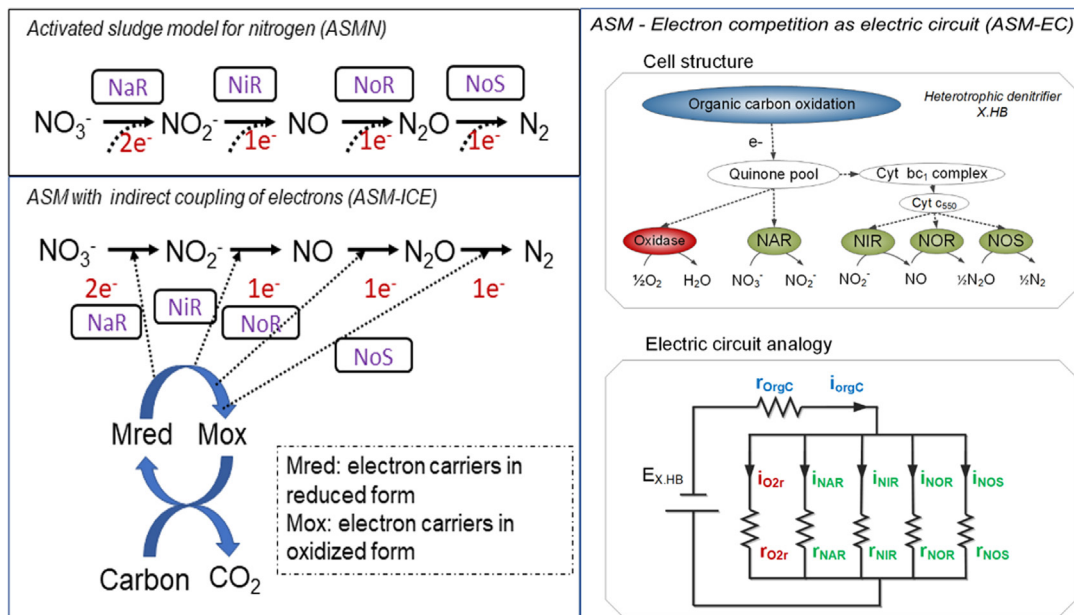


**Figure 7.1** Schematic illustration of denitrification models. ASMN: [Hiatt and Grady \(2008\)](#); ASM-ICE: [Pan \*et al.\* \(2013b\)](#); ASM-EC electric circuit analogy: [Domingo-Félez and Smets \(2020a\)](#).

model describes each of the four steps as a separate and independent oxidation-reduction reaction (Table S2 in SI), with the kinetics of each step modelled according to the nitrogen reduction reaction kinetics and using a stoichiometric relationship obtained through an electron balance. Model OHO-A ignores the fact that the nitrogen oxides reduction and carbon oxidation are carried out by different enzymes with their specific kinetics, and consequently either of the two processes could limit the rate of denitrification. In addition, this coupling approach describes each denitrification step independently with its rate not being affected by other denitrification steps that draw electrons from the same electron supply. Essentially, the carbon oxidation rate is modelled as the sum of the carbon requirements by all denitrification steps, with the underlying assumption that electron supply will always be able to meet the predicted total electron demand.

This model's structure is close to what wastewater modellers are used to, that is kinetics depending on soluble and particulate components, and less on detailed metabolic pathway information. The importance of  $N_2O$  accumulation and emission logically depend on respective consumption and production rates. For instance it could be mentioned that this model predicts more  $N_2O$  production in the case of organic matter limitation by using a higher  $K_s$  value for organic matter in the last reaction (original set of parameter values by [Hiatt and Grady, 2008](#)). This is an important point in terms of acceptability and usability in the profession.

### 7.2.1.3 Activated sludge model with indirect coupling of electrons (ASM-ICE)

The 'indirect coupling approach', proposed by [Pan \*et al.\* \(2013b\)](#) and named ASM-ICE, decouples the carbon oxidation and nitrogen reduction processes. Electron carriers are introduced as a new component in this model to link carbon oxidation to nitrogen oxides reduction, in which carbon oxidation reduces carriers and nitrogen oxides reduction oxidizes carriers (Model OHO-B in [Table 7.1, Pan \*et al.\*, 2013b](#)). In this way, each step of heterotrophic denitrification can be regulated by

Table 7.1 Key differences among the N<sub>2</sub>O models by heterotrophs, single-pathway models by AOB and two-pathway models by AOB

N <sub>2</sub> O models	Model components	Stoichiometric	Kinetic	Reference
N <sub>2</sub> O models by heterotrophs	Model OHO-A	Without electron carriers.	Without electron competition concept.	Hiatt and Grady (2008)
	Model OHO-B	With electron carriers.	With electron competition concept.	Pan <i>et al.</i> (2013b)
Single-pathway models by AOB	Model A – AOB denitrification	Using SNH <sub>4</sub> and SNO <sub>2</sub> ; With SNH <sub>2</sub> OH.	Two different oxygen affinity constants; Oxygen inhibition on NO <sub>2</sub> <sup>-</sup> and NO reductions; Anoxic reduction factor.	Ni <i>et al.</i> (2011)
	Model A1 – AOB denitrification	Using SNH <sub>3</sub> and SHNO <sub>2</sub> ; With SNH <sub>2</sub> OH.	Two different oxygen affinity constants; Without oxygen inhibition; NH <sub>3</sub> inhibition on NH <sub>3</sub> oxidation; Anoxic reduction factor.	Pocquet <i>et al.</i> (2013)
Model B – AOB denitrification	Using SNH <sub>3</sub> and SHNO <sub>2</sub> ; Without SNH <sub>2</sub> OH.	One-step NH <sub>4</sub> <sup>+</sup> oxidation; Two-step NO <sub>2</sub> <sup>-</sup> reduction; Cell growth during all 3 processes.	Only one oxygen affinity constant; Without oxygen inhibition; Anoxic reduction factor.	Mampaey <i>et al.</i> (2013)
		Same as Model B.	Only one oxygen affinity constant; NH <sub>3</sub> and HNO <sub>2</sub> inhibitions on NH <sub>3</sub> oxidation; Haldane function for oxygen limitation/inhibition; Anoxic reduction factor.	Guo and Vanrolleghem (2014)
Model C – NH <sub>2</sub> OH pathway (via NOH)	Using SNH <sub>4</sub> and SNO <sub>2</sub> ; With SNOH.	Three-step NH <sub>4</sub> <sup>+</sup> oxidation via NOH; Cell growth during NH <sub>2</sub> OH oxidation.	Two different oxygen affinity constants; NOH breakdown to produce N <sub>2</sub> O.	Law <i>et al.</i> (2012)
		Three-step NH <sub>4</sub> <sup>+</sup> oxidation via NO; Cell growth during NH <sub>2</sub> OH oxidation.	Two different oxygen affinity constants; NO reduction to produce N <sub>2</sub> O; Without oxygen inhibition.	Ni <i>et al.</i> (2013b)

(Continued)

**Table 7.1** Key differences among the N<sub>2</sub>O models by heterotrophs, single-pathway models by AOB and two-pathway models by AOB (Continued).

N <sub>2</sub> O models	Model components	Stoichiometric	Kinetic	Reference
Two-pathway models by AOB	Model E Using SNH <sub>4</sub> and SNO <sub>2</sub> ; With electron carriers.	Three-step NH <sub>4</sub> <sup>+</sup> oxidation; One-step NO <sub>2</sub> <sup>-</sup> reduction; Without cell growth.	Applying electron competition concept; Without oxygen inhibition; Without anoxic reduction factor.	Ni <i>et al.</i> (2014)
	Model F Mostly same as Model E; With SCO <sub>2</sub> ; With energy carriers.	Mostly same as Model E; With energy carriers involved; With cell growth considered.	Mostly same as Model E; With energy carriers involved; With effect of inorganic carbon considered.	Peng <i>et al.</i> (2015a)
	Model G Using SNH <sub>3</sub> and SHNO <sub>2</sub> With SNH <sub>2</sub> OH.	Two-step NH <sub>3</sub> oxidation; One-step HNO <sub>2</sub> reduction; Cell growth during NH <sub>2</sub> OH oxidation.	With oxygen inhibition of denitrification; With reduction factor; Three different oxygen affinity constants.	Pocquet <i>et al.</i> (2016)
	Model H Using SNH <sub>3</sub> and SHNO <sub>2</sub> With SNH <sub>2</sub> OH.	Two-step NH <sub>3</sub> oxidation; Two-step HNO <sub>2</sub> reduction; Cell growth during NH <sub>2</sub> OH oxidation; O <sub>2</sub> -independent NH <sub>2</sub> OH oxidation.	With oxygen inhibition of denitrification; With reduction factor; Two different oxygen affinity constants; Two different NH <sub>2</sub> OH affinity constants.	Domingo-Félez and Smets (2016)

both the nitrogen reduction and the carbon oxidation processes. The possibility of either the carbon oxidation or electron transfer being a limiting step in denitrification is thus considered in the model. In heterotrophic denitrifiers, competition for electrons may occur between the four reduction steps when the electron supply rate from the oxidation process cannot meet the demand for electrons from the four reduction steps (Pan *et al.*, 2013b), which plays an important role in the accumulation and emission of N<sub>2</sub>O (Pan *et al.*, 2013a). The electron competition between the four denitrifying steps can be modelled by assigning different values to the affinity constants responsible for Processes 2, 3, 4 and 5 with respect to M<sub>red</sub>, which are provided by Process 1. Model OHO-B can be used as a practical tool for predicting N<sub>2</sub>O accumulation during denitrification, with the complex biochemical reactions and electron transfer processes involved in biological denitrification by different microbial species being lumped into one oxidation and four reduction reactions that are linked through electron carriers.

#### 7.2.1.4 Activated sludge model – electron competition (ASM-EC)

Almeida *et al.* (1997) proposed that the electron flow through the respiratory chain can be modelled similarly to electron flow across resistors in an electric circuit. A model structure describing four-step denitrification, aerobic respiration, and organic carbon oxidation was proposed using the analogy between electron competition during respiration and electron distribution in a multi-resistor electric circuit (Domingo-Félez and Smets, 2020a). A potential is created by the presence of heterotrophic denitrifying bacteria that mediate electron transfer between an electron donor and an electron acceptor pair. The competition for electrons between multiple denitrifying enzymes is analogous to the electron flow through parallel resistors. Reaction rates are analogous to the current intensity through a resistor (Ohm's law). Individual resistances vary with the substrate concentrations, and the electron current released through electron donor (i.e., organic substrates) oxidation will be distributed between reduction rates. Following conservation of potential and conservation of charge, the current through any resistor can be calculated. The ASM–EC model can substitute the process rates describing denitrification in ASM-type models and includes fewer parameters than ASMN or ASM-ICE.

### 7.2.2 Modelling N<sub>2</sub>O production by AOB

#### 7.2.2.1 Introduction

AOB are chemolithotrophs that oxidize ammonia (NH<sub>3</sub>) to nitrite (NO<sub>2</sub><sup>-</sup>) via hydroxylamine (NH<sub>2</sub>OH) as their predominant energy-generating metabolism (Arp and Stein, 2003; Arp *et al.*, 2007) (Figure 7.2a). The first step is catalysed by ammonia monooxygenase (AMO) where NH<sub>3</sub> is oxidized to NH<sub>2</sub>OH with the reduction of molecular oxygen (O<sub>2</sub>). In the second step, NH<sub>2</sub>OH is oxidized to NO<sub>2</sub><sup>-</sup> by hydroxylamine oxidoreductase (HAO), with O<sub>2</sub> as the primary electron acceptor. However, AOB contain a periplasmic copper-containing nitrite reductase (NirK) and a nitric oxide reductase (Nor) (Chandran *et al.*, 2011; Hooper *et al.*, 1997) (as shown in Figure 7.2a). NirK could speed up NH<sub>2</sub>OH oxidation by channelling electrons from the cytochrome pool to NO<sub>2</sub><sup>-</sup> (to form NO) and thus play a facilitative role in NH<sub>3</sub> oxidation itself (Chandran *et al.*, 2011; Hooper *et al.*, 1997). AOB also possess the inventory to alternatively convert NO into N<sub>2</sub>O, using a haem–copper nitric oxide reductase, sNOR (Chandran *et al.*, 2011).

Although N<sub>2</sub>O is not an obligate intermediate in NH<sub>3</sub> oxidation, N<sub>2</sub>O can be produced by AOB through two major pathways according to the current understanding (Figure 7.2a): (i) N<sub>2</sub>O as a by-product of incomplete oxidation of NH<sub>2</sub>OH to NO<sub>2</sub><sup>-</sup>, typically referred to as the NH<sub>2</sub>OH oxidation pathway (Chandran *et al.*, 2011; Law *et al.*, 2012; Poughon *et al.*, 2000; Stein, 2011a), and (ii) N<sub>2</sub>O as the final product of AOB denitrification with NO<sub>2</sub><sup>-</sup> as the terminal electron acceptor and NO as an intermediate, the so-called nitrifier or AOB denitrification pathway (Chandran *et al.*, 2011; Ni *et al.*, 2013b; Stein, 2011b).

It is generally accepted that NO<sub>2</sub><sup>-</sup> and NO reduction for N<sub>2</sub>O production is carried out by AOB under oxygen limiting or completely anoxic conditions (Kampschreur *et al.*, 2009; Law *et al.*, 2013). Increased N<sub>2</sub>O production under high NO<sub>2</sub><sup>-</sup> concentrations has been suggested to be due to AOB

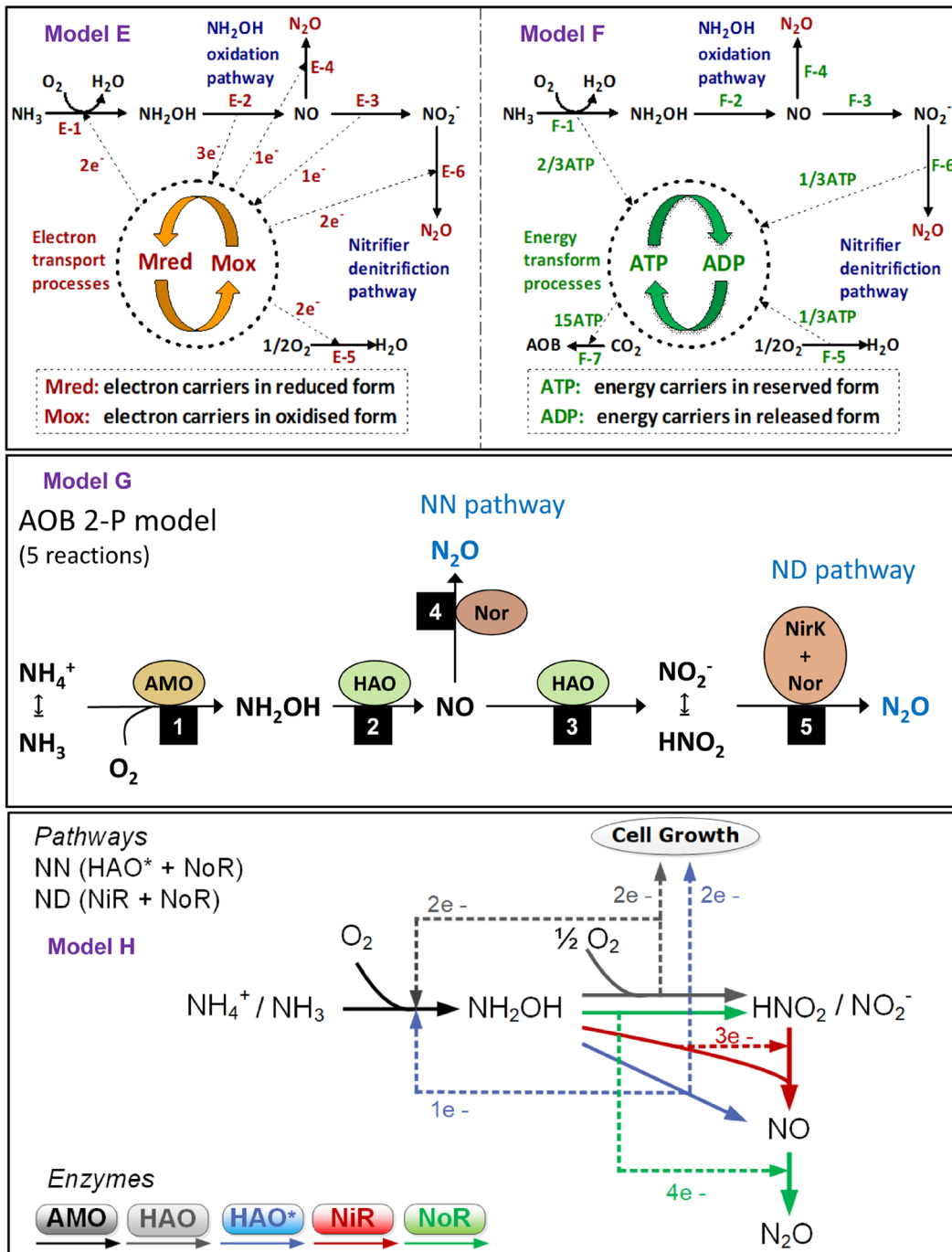


Figure 7.2 General description of the two-pathway AOB models (E: Ni *et al.*, 2014, F: Peng *et al.*, 2015a, G: Pocquet *et al.*, 2016; H: Domingo-Félez and Smets, 2016). NN: hydroxylamine pathway, ND: nitrifier denitrification pathway.

denitrification (Yang *et al.*, 2009; Yu *et al.*, 2010). On the other hand, there is also evidence supporting N<sub>2</sub>O production from NH<sub>2</sub>OH oxidation by AOB. The higher NH<sub>3</sub> oxidation rate could result in the accumulation of NH<sub>2</sub>OH and other reaction intermediates such as NO or NOH (Law *et al.*, 2012), which in turn result in N<sub>2</sub>O formation with detailed reactions yet to be fully elucidated (Chandran *et al.*, 2011; Stein, 2011a).

As the fundamental metabolic pathways for N<sub>2</sub>O production by AOB are now coming to light (Castro-Barros *et al.*, 2015; Harris *et al.*, 2015; Kampschreur *et al.*, 2007; Okabe *et al.*, 2011; Perez-García *et al.*, 2014; Schreiber *et al.*, 2009; Stein, 2011a; Yu *et al.*, 2010), several mechanistic models have been proposed for N<sub>2</sub>O production by AOB in mixed culture based on one or two of the known N<sub>2</sub>O production pathways of AOB, that is AOB denitrification and NH<sub>2</sub>OH oxidation pathways. To date, two categories of N<sub>2</sub>O production models by AOB in mixed culture have been proposed, which are represented by single-pathway models and two-pathway models.

### 7.2.2.2 Single-pathway models

Six different single-pathway model structures available in literature are presented in Table S3 in the SI, detailed with their kinetic and stoichiometric matrices. Table 7.1 presents the key differences among the model structures of these single-pathway models by AOB.

Model A (Ni *et al.*, 2011) and Model B (Mampaey *et al.*, 2013) are based on the AOB denitrification pathway. In Model A (Table 7.1, Ni *et al.*, 2011), AOB denitrification with NO<sub>2</sub><sup>-</sup> as the terminal electron acceptor produces NO and subsequently N<sub>2</sub>O by consuming NH<sub>2</sub>OH as the electron donor. Similarly, in Model B (Table 7.1, Mampaey *et al.*, 2013), AOB denitrification occurs in parallel with ammonium oxidation, reducing NO<sub>2</sub><sup>-</sup> to NO and then to N<sub>2</sub>O with ammonium as the electron donor. The key difference between these two models is that in Model A, dissolved oxygen (DO) is assumed to inhibit nitrite and NO reduction by AOB, while in Model B, this inhibition is absent. A further minor difference is that ammonia oxidation is modelled as a two-step (ammonia to hydroxylamine and then to nitrite) process in Model A, but as a one-step process (ammonia to nitrite) in Model B.

Model A1 (Pocquet *et al.*, 2013) and Model B1 (Guo and Vanrolleghem, 2014) are also based on the AOB denitrification pathway, and are the two modified versions of Models A and B which describe N<sub>2</sub>O production in several studies (Guo and Vanrolleghem, 2014; Pocquet *et al.*, 2013). In Model A1 (Table 7.1, Pocquet *et al.*, 2013), the oxygen inhibition of the AOB denitrification pathway was removed. In addition, free ammonia (FA) and free nitrous acid (FNA) were considered as the substrate for the AOB reactions, in order to explicitly consider the effect of pH variation. In Model B1 (Table 7.1, Guo and Vanrolleghem, 2014), oxygen limitation and inhibition was added through a Haldane function in the kinetics of both nitrite reduction and NO reduction processes (Guo and Vanrolleghem, 2014). Inhibition by FA was also considered in Model A1 and inhibition by both FA and FNA were included in Model B1.

Model C (Law *et al.*, 2012) and Model D (Ni *et al.*, 2013b) are based on the NH<sub>2</sub>OH oxidation pathway. Model C assumes that N<sub>2</sub>O production is due to the chemical decomposition of the unstable NOH, an intermediate of NH<sub>2</sub>OH oxidation (Law *et al.*, 2012). In contrast, Model D assumes that the reduction of NO, produced from the oxidation of NH<sub>2</sub>OH, resulted in N<sub>2</sub>O production by consuming NH<sub>2</sub>OH as the electron donor. Model D (Table 7.1, Ni *et al.*, 2013b) assumes that DO has no inhibitory effect on NO reduction (Yu *et al.*, 2010), as in Model B.

### 7.2.2.3 Two-pathway models

The two N<sub>2</sub>O production pathways of AOB (NN: hydroxylamine pathway, ND: nitrifiers denitrification) have been integrated into different two-pathway models. Table 7.1 and Figure 7.2 compare the key differences between these four models (E–H). Two of them (E–F) are based on the decoupling approach with electron carriers (Ni *et al.*, 2014; Peng *et al.*, 2015a) whereas the two others (G–H) are based on the coupling approach (Domingo-Félez and Smets, 2016; Pocquet *et al.*, 2016).

In Model E (Table 7.1, Ni *et al.*, 2014), the complex biochemical reactions and electron transfer processes involved in AOB metabolism are lumped into three oxidation and three reduction reactions (Figure 7.2). Electron carriers are introduced as a new component in the model to link the electron transfer from oxidation to reduction. By decoupling the oxidation (E-1 to E-3 in Figure 7.2) and reduction (E-4 to E-6 in Figure 7.2) reactions through the use of electron carriers, the electron distribution between O<sub>2</sub>, NO<sub>2</sub><sup>-</sup> and NO as electron sinks is modelled by assigning different kinetic values to Processes E-4, E-5 and E-6 with respect to electron carriers. These electron carriers are regenerated by Processes E-2 and E-3. In this way, the model can predict the relative contribution of the two pathways to total N<sub>2</sub>O production by AOB, as well as the shifts in the dominating pathway at various DO and nitrite level conditions.

Model F (Peng *et al.*, 2015a) is based on the decoupling approach with both electron and energy (adenosine triphosphate) balances, which are proposed by the extension of Model E to describe the dependency of N<sub>2</sub>O production by AOB on the inorganic carbon (IC) concentration (Peng *et al.*, 2015a). In addition to the electron carriers that link electron transfer from oxidation to reduction, adenosine triphosphate (ATP)/adenosine diphosphate (ADP) are also introduced as components in the model (Table 7.1) to link energy generation to IC fixation for biomass growth (Figure 7.2). The energy distribution between ammonia oxidation, NO<sub>2</sub><sup>-</sup> reduction and oxygen reduction as energy source (ATP) is modelled through assigning different kinetic values to Processes F-1, F-5 and F-6 with respect to ADP, which is consumed by Process F-7 with IC as substrate for AOB growth. In this way, the possible effect of IC on AOB growth, and subsequently the N<sub>2</sub>O production from different pathways by AOB, can be explicitly described when the IC concentration in the bioreactor varies temporally or spatially, with N<sub>2</sub>O production increasing with an increase in IC concentrations.

In Model G (Table 7.1, Pocquet *et al.*, 2016) the two pathways are combined based on a direct coupling approach. The model includes five enzymatic reactions (Figure 7.2). As in models E and F, NO is considered as an intermediary compound during oxidation of hydroxylamine into nitrite and N<sub>2</sub>O is supposed to be produced by both the reduction of NO (hydroxylamine pathway) and the reduction of nitrite (AOB denitrification). Free ammonia and free nitrous acid are considered as substrate for nitrification and denitrification, respectively. As in model E and F, the NO intermediary is not considered in the denitrification pathway which avoids the NO loop (i.e., production via nitrite reduction and re-oxidation into nitrite). The inhibition of AOB denitrification by oxygen is considered by a modified Haldane equation as in Guo and Vanrolleghem (2014).

In Model H (Table 7.1, Domingo-Félez and Smets, 2016) the two pathways are also combined based on a direct coupling approach and it includes five enzymatic reactions (Figure 7.2). Free ammonia and free nitrous acid are considered the substrates for nitrification and denitrification, respectively. Hydroxylamine is oxidized aerobically producing nitrite and is independent of oxygen presence producing NO (hydroxylamine pathway). The inhibition of AOB denitrification by oxygen is considered by an inverse Michaelis-Menten-like equation and produces NO (AOB denitrification). Hence, NO is an intermediate of the two pathways with different dependencies on oxygen and free nitrous acid concentrations. A single autotrophic N<sub>2</sub>O-producing process accounts for the combined NO reduction.

## 7.3 MODEL INTEGRATION, USE AND CALIBRATION

### 7.3.1 Integrated N<sub>2</sub>O models

N<sub>2</sub>O can be generally produced by both AOB and heterotrophic denitrifiers in WWTPs and consumed by heterotrophic denitrifiers (Guo and Vanrolleghem, 2014; Kampschreur *et al.*, 2009; Law *et al.*, 2012). Therefore, integrated N<sub>2</sub>O models incorporating N<sub>2</sub>O production/consumption by both AOB and heterotrophic denitrifiers would contribute to more powerful models that predict the N<sub>2</sub>O dynamics more accurately in WWTPs, which could also be a useful tool for the development of N<sub>2</sub>O mitigation strategies.

Two approaches have been reported to integrate the N<sub>2</sub>O production/consumption by both AOB and heterotrophic denitrifiers into a comprehensive N<sub>2</sub>O model: (i) ASM-type models that combine one of the single-pathway models of AOB (e.g., Models A–D, Table S3) with ASMN of heterotrophic denitrifiers (Model OHO-A, Table S2) (Guo and Vanrolleghem, 2014; Ni *et al.*, 2011; Pocquet *et al.*, 2013; Spérandio *et al.*, 2016), and (ii) electron balance-based models that integrate the electron carrier-based two-pathway model of AOB (Model E, Table S4) and ASMN (Model OHO-A, Table S2) (Ni *et al.*, 2015). Both modelling approaches have been successfully applied to describe N<sub>2</sub>O emissions from mixed culture nitrification-denitrification systems and to identify the relative contributions of AOB and heterotrophic denitrifiers to total N<sub>2</sub>O production (Ni *et al.*, 2011, 2013b, 2015; Spérandio *et al.*, 2016). A third potential approach to integrate the N<sub>2</sub>O production/consumption by both AOB and heterotrophic denitrifiers could be a full electron balance-based model integrating the electron carrier-based two-pathway model of AOB (Model E, Table S4) and the electron carrier-based model of heterotrophs (Model OHO-B, Table S2), this requires future testing though. Model H integrates a two-pathway AOB model, ASMN of heterotrophic denitrifiers and abiotic reactions considering free nitrous acid and hydroxylamine.

It should be noted that the possible consumption of N<sub>2</sub>O by heterotrophic denitrification as an N<sub>2</sub>O sink may occur and reduce overall N<sub>2</sub>O production in an integrated model under the conditions of high COD to N ratio and/or low DO level.

### 7.3.2 Model Evaluation against experimental data

The N<sub>2</sub>O models have to be tested to predict N<sub>2</sub>O emission data from experiments in order for the models to become useful tools in practical applications. During recent years, many measurement campaigns have been performed. All available N<sub>2</sub>O models have been evaluated with experimental data collected from different systems to reveal their performance under various process conditions and shed light on the conditions under which each of the models would be suitable for application.

#### 7.3.2.1 Heterotrophic denitrification

For denitrifying N<sub>2</sub>O models, Model OHO-A was found generally able to reproduce the nitrate, nitrite and N<sub>2</sub>O profiles when only one nitrogen oxide species was added (Ni *et al.*, 2011; Pan *et al.*, 2015), but Model OHO-A failed to reproduce the results when two or more nitrogen oxide species were added together. In contrast, Model OHO-B was shown to be able to describe general COD consumption, nitrate reduction and nitrite accumulation by an enriched denitrifying culture (Pan *et al.*, 2015), and the influence of nitrite and N<sub>2</sub>O addition on nitrate reduction, as well as the experimental results when one or more nitrogen oxide species were added (Pan *et al.*, 2015). Therefore the decoupling approach of Model OHO-B might be essential to describe complex conditions with addition of multiple nitrogen oxide species, but in the many situations for which only nitrate and nitrite are provided Model OHO-A is still applicable. For both models it can be noted that an independent calibration of each of the successive steps of denitrification has rarely been possible. As heterotrophic denitrification is an important N<sub>2</sub>O mechanism to be considered for future mitigation strategies, more measurements of intermediates is recommended in future studies to improve the robustness of the models calibration.

#### 7.3.2.2 Single-pathway AOB models

The six single-pathway AOB models (Models A–D, Table 7.1) were evaluated and compared (Ni *et al.*, 2011, 2013a; Spérandio *et al.*, 2016) based on their ability to capture the observed N<sub>2</sub>O production results from different experiments (Kim *et al.*, 2010; Law *et al.*, 2012; Spérandio *et al.*, 2016; Yang *et al.*, 2009). Model A could predict well the observed trend of a decrease in N<sub>2</sub>O production at high DO concentrations (Yang *et al.*, 2009), whereas Model B was not able to predict such a trend due to the absence of oxygen inhibition on AOB denitrification in Model B (Ni *et al.*, 2013a). Model B could not describe well the N<sub>2</sub>O peak that is likely related to the dynamics of NH<sub>2</sub>OH (Ni *et al.*, 2013a), which was not included in Models B and B1. Models A, A1, B and B1 have been tested and found to

reasonably describe  $N_2O$  production data with high nitrite accumulation (Figure 7.3) (Pocquet *et al.*, 2013; Spérandio *et al.*, 2016). In contrast, both Models C and D were not able to capture the observed dependency of  $N_2O$  production on nitrite availability (Kim *et al.*, 2010; Spérandio *et al.*, 2016; Yang *et al.*, 2009) due to the fact that the two models are linked to incomplete  $NH_2OH$  oxidation. However, Models C and D were able to reproduce the experimental observations that the  $N_2O$  production increased/decreased with increasing/decreasing DO concentration (Law *et al.*, 2012). The kinetic structure of Model B also ensured that the  $N_2O$  production rate was dependent on oxygen availability, resulting in a similar  $N_2O$  dynamic trend (increase in the  $N_2O$  production rate with an increase in DO concentration). On the contrary, Model A predicted the opposite to such an observation (Law *et al.*, 2012). These results suggest that DO inhibition might be required to describe AOB denitrification and  $NH_2OH$  needs to be included as a necessary intermediate. The use of FA and FNA in model structures would be recommended for a better description of the pH effect and possible FNA inhibition. NOH would be preferably used as an  $N_2O$  precursor for describing the  $NH_2OH$  pathway under extremely high nitrite accumulation conditions, whereas NO could be generally applied as an intermediate for  $N_2O$  production from  $NH_2OH$  oxidation under common wastewater conditions.

### 7.3.2.3 Two-pathway AOB models

With respect to the two-pathway models of AOB, Model E has satisfactorily described the  $N_2O$  data from several different nitrifying cultures (partial nitrification culture or/and full nitrification culture) and under various DO and  $NO_2^-$  concentration conditions (Figure 7.4) (Ni *et al.*, 2014; Peng *et al.*, 2014; Sabba *et al.*, 2015). Model F has also predicted well these different nitrifying cultures (partial nitrification and full nitrification culture) but also under various IC conditions (Peng *et al.*, 2015a). Although the electron-based two-pathway models (Models E and F) have been demonstrated to be effective, electron carriers may not necessarily be the only approach to the integration of the two

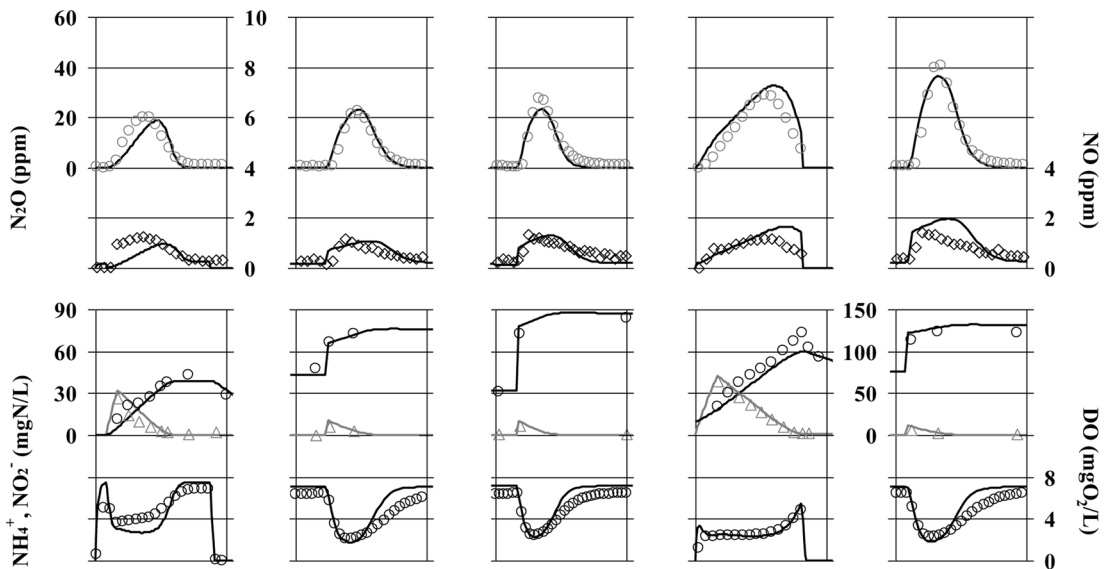


**Figure 7.3** Comparison of simulation (A1, Pocquet *et al.*, 2013) and measured data for five batch experiments at different nitrite and ammonium levels. NO in gas phase ( $\diamond$ ),  $N_2O$  in gas phase ( $\circ$ ), ammonium ( $\Delta$ ), nitrite ( $\square$ ) and dissolved oxygen ( $\square$ ). Duration of experiments: 1 h.  $N_2O$  emission factors: 1.39%, 2.58%, 3.86%, 1.83%, 4.52% ( $gN-N_2O/gN-NH_4^+$ ), respectively (Spérandio *et al.*, 2016).

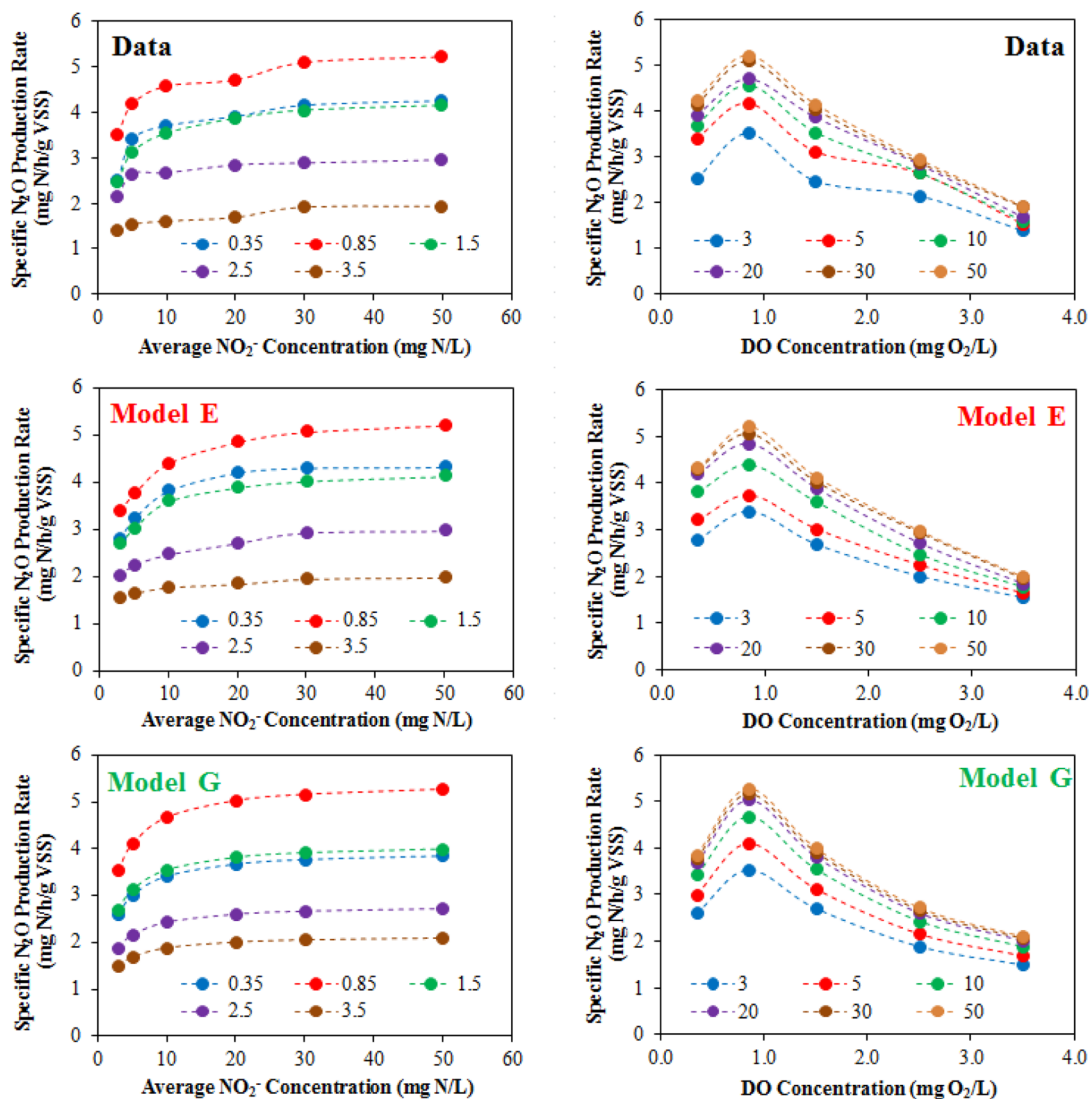


**Figure 7.4** Comparison of Model E and Model G predictions (two-pathway models). Experimental and simulated effect of dissolved oxygen and nitrite concentrations on specific N<sub>2</sub>O production rate during short-term (batch) experiments (Lang *et al.*, 2017).

pathways into one model. Model G is based on the *coupling approach* without considering electron carriers. It was calibrated with batch experiments and validated with long-term data collected in a sequencing batch reactor performing nitrification and denitrification (Pocquet *et al.*, 2016; Mampaey *et al.*, 2019). A good prediction of the N<sub>2</sub>O emissions for varying nitrite concentrations was obtained. Model G is also capable of describing the trends observed for the NO emissions and the variation of the NO/N<sub>2</sub>O ratio depending on the pathways' contribution. The combined effect of nitrite (via free nitrous acid) and dissolved oxygen (DO) is also correctly predicted by Model G (Figure 7.4) (Lang *et al.*, 2017).

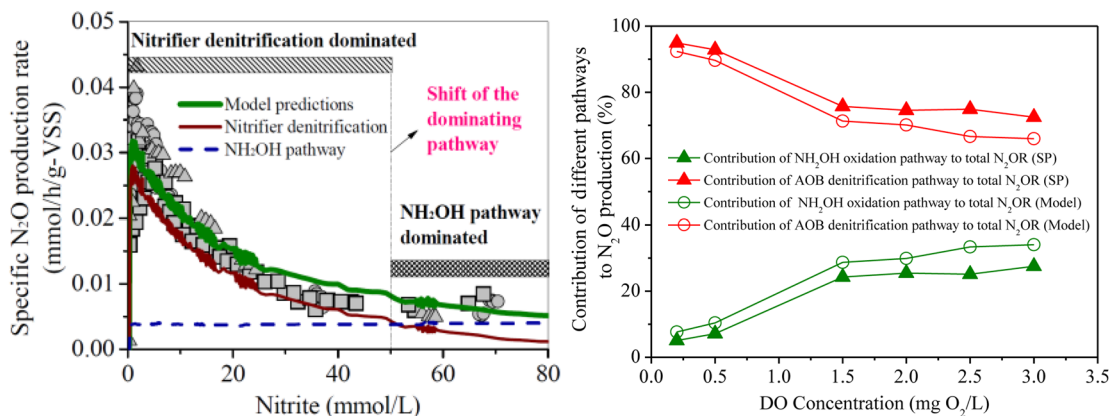


**Figure 7.5** Predicted contributions from the nitrifier denitrification pathway and the  $NH_2OH$  pathway as well as their shifts using Model E (real data: symbols, model predictions: lines) for a partial nitrification (left panel adapted from Ni *et al.*, 2014) and a full nitrification system (right panel adapted from Peng *et al.*, 2014).

Two-pathway models E and G successfully predicted shifts of the dominating pathway at various DO, nitrite and/or IC levels (see Figure 7.5, Lang *et al.*, 2017), consistent with experimental observations that  $N_2O$  was produced from both nitrifier denitrification and  $NH_2OH$  oxidation pathways by AOB (Ni *et al.*, 2014; Peng *et al.*, 2014; Wunderlin *et al.*, 2013). The model results suggested that the contribution of AOB denitrification decreased as DO increased, accompanied by a corresponding increase in the contribution by the  $NH_2OH$  oxidation pathway. This was verified by site preference (SP) isotopic measurements (Peng *et al.*, 2014). The two-pathway models also successfully predicted the increase of the AOB denitrification pathway with nitrite (at low nitrite concentrations) and the inhibition of AOB denitrification at high nitrite concentrations (see Figure 7.5) (Ni *et al.*, 2014; Pocquet *et al.*, 2016).

Model H was calibrated with AOB-enriched biomass and activated sludge mixed liquor biomass (Domingo-Félez and Smets, 2020b; Domingo-Félez *et al.*, 2017; Su *et al.*, 2019b). Optimal extant respirometry and anaerobic batch experiments that target endogenous and exogenous processes (of both autotrophic ammonium/nitrite oxidation and heterotrophic denitrification), together with the associated net  $N_2O$  production were designed and executed. The calibrated model predicts the NO and  $N_2O$  dynamics at varying ammonium, nitrite and dissolved oxygen levels in the two independent systems.

### 7.3.3 Selection of models for $N_2O$ Prediction

#### 7.3.3.1 Single-pathway AOB models versus two-pathway AOB models

The model evaluation results strongly suggest that appropriate selection of available  $N_2O$  models is important for accurate  $N_2O$  prediction in different engineering nitrogen removal systems under different operational conditions. Figure 7.6 presents a possible guideline for model selection in their further applications.

For  $N_2O$  production by heterotrophic denitrifiers, Model OHO-A can be used to predict the overall nitrogen and COD removal performance in a wastewater treatment plant, as in most cases the low level accumulation of denitrification intermediates does not significantly affect the overall nitrogen removal rate. However, in the context of predicting the  $N_2O$  production by heterotrophic denitrifiers, Model OHO-B is inadequate due to its structural deficiency in describing the electron competition process in denitrification. Model H enhanced our ability to predict  $N_2O$  production by heterotrophic denitrifiers and has the potential to describe all  $N_2O$  data under different conditions. However, it

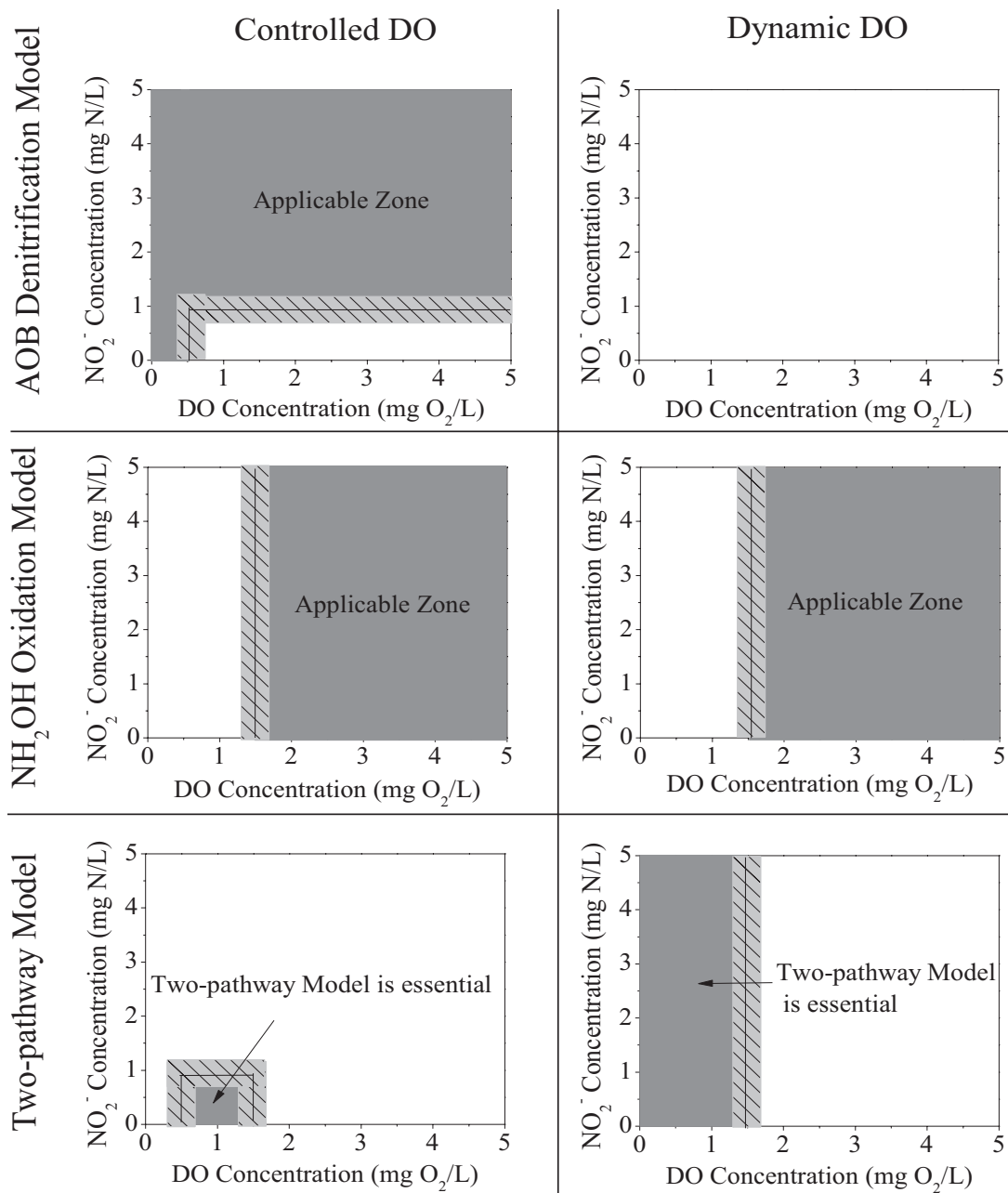


**Figure 7.6** Summary of applicable regions for the AOB denitrification model, the NH<sub>2</sub>OH oxidation model and the two-pathway model under various DO and NO<sub>2</sub><sup>-</sup> concentrations. The applicable regions were insensitive to the variations of key parameters governing N<sub>2</sub>O production by the two-pathway model (Peng *et al.*, 2015b).

**Table 7.2** Guideline for model selection for predicting N<sub>2</sub>O production by AOB and heterotrophic denitrification

N <sub>2</sub> O models	Single-pathway models by AOB	Two-pathway models by AOB	N <sub>2</sub> O models by heterotrophs
Applicable conditions	<ul style="list-style-type: none"> <li>Models A, A1, B and B1 to describe the regulation of N<sub>2</sub>O production by nitrite (or FNA)</li> <li>Model A to predict possible DO inhibition on N<sub>2</sub>O production at high DO levels</li> <li>Models A1, B and B1 to predict possible pH effect and FA/FNA inhibition on N<sub>2</sub>O production</li> <li>Models C and D to describe N<sub>2</sub>O emissions at high DO levels and low nitrite accumulation</li> </ul>	<ul style="list-style-type: none"> <li>Model E to predict N<sub>2</sub>O production at varying DO and NO<sub>2</sub><sup>-</sup> with constant IC</li> <li>Model F to describe N<sub>2</sub>O production under highly dynamic IC condition</li> <li>Model G to predict NO and N<sub>2</sub>O production at varying DO and NO<sub>2</sub><sup>-</sup> and possible pH and FA/FNA effects on N<sub>2</sub>O production</li> </ul>	<ul style="list-style-type: none"> <li>Model OHO-A to predict the overall nitrogen and COD removal performance with low level accumulation of denitrification intermediates</li> <li>Model OHO-B to describe N<sub>2</sub>O production under different conditions</li> </ul>
Inabilities of the models	<ul style="list-style-type: none"> <li>Model A not to describe the increase of N<sub>2</sub>O production with increasing DO</li> <li>Models B and B1 not to predict the N<sub>2</sub>O production related to the dynamics of NH<sub>2</sub>OH</li> <li>Models C and D not to predict the effect of nitrite accumulation on N<sub>2</sub>O production</li> </ul>	<ul style="list-style-type: none"> <li>Model E and G not to describe N<sub>2</sub>O production with dynamic IC</li> <li>Model E and F not to describe pH effect on N<sub>2</sub> production</li> <li>Model E and F not to describe NO production</li> </ul>	<ul style="list-style-type: none"> <li>Model OHO-A not to describe N<sub>2</sub>O production with electron competition</li> </ul>
Key parameters for calibration	<ul style="list-style-type: none"> <li>The half saturation constant for nitrite or FNA (<math>K_{NO_2, AOB}</math> or <math>K_{HNO_2, AOB}</math> for Models A, A1, B, B1)</li> <li>The reduction factor for N<sub>2</sub>O production (<math>\eta_{AOB}</math>, for all six single-pathway models)</li> </ul>	<ul style="list-style-type: none"> <li>E, F: The affinity constants with respect to electrons (e.g., <math>K_{Mred,3r}</math> and <math>K_{Mred,4}</math>)</li> <li>E, F: The ratios among the affinity constants to electrons</li> <li>G, H: The reduction factors, affinity constant for HNO<sub>2</sub> and NH<sub>2</sub>OH</li> </ul>	<ul style="list-style-type: none"> <li>The N<sub>2</sub>O production and reduction rates</li> <li>The relative ratios between electron affinity constants</li> </ul>

requires information on both the carbon oxidation reaction kinetics and the nitrogen reduction kinetics.

For N<sub>2</sub>O production by AOB, the single-pathway models (Models A–D) have simpler structures (one single pathway involved) and fewer parameters, which is convenient for model calibration (Table 7.2). This makes their use preferential under certain conditions, even though they may not be able to reproduce all N<sub>2</sub>O data. The two-pathway models (Models E–G) have the potential to describe all N<sub>2</sub>O data with different operational conditions, but may require more efforts in model calibration because of their larger number of parameters. Specifically (Table 7.2), Models A, A1, B and B1 might be used to describe the regulation of N<sub>2</sub>O production by nitrite (or FNA) concentrations. Models C and D might be able to describe N<sub>2</sub>O emissions from systems under relatively high DO concentrations and low nitrite accumulation that likely favour the NH<sub>2</sub>OH oxidation pathway for N<sub>2</sub>O production. In addition, according to the analysis by Peng *et al.* (2015b) (Figure 7.6), for the AOB denitrification model to be used (e.g., Model A) it is preferable that the DO concentration in the system is well controlled at a constant level. NH<sub>2</sub>OH oxidation models (e.g., Model D) can be applied under high DO conditions.

Under other conditions, the two-pathway models (e.g., Model E or G) should be applied. Model E or Model G could be used under varying DO and NO<sub>2</sub><sup>-</sup> concentrations, but stable IC conditions are required, while Model F would be preferable under highly dynamic IC conditions.

### 7.3.3.2 Two-pathway AOB models: direct versus indirect coupling approach

The two different two-pathway models E and G based on indirect coupling or direct coupling approaches, respectively, were compared by Lang *et al.* (2017). Both were calibrated to describe the experimental N<sub>2</sub>O emissions collected from 43 kinetic experiments considering a large range for both DO and nitrite concentrations and three different AOB-enriched cultures (Lang *et al.*, 2017) (Figure 7.4).

Both models enabled the prediction that the increase of DO enhances the hydroxylamine pathway contribution while it reduces the contribution of the AOB denitrification pathway (Figure 7.7). This is related to competition between oxygen and nitrite for electron carriers in Model E, whereas it is described by an inhibition term in the AOB denitrification kinetics in Model G. Regarding the nitrite effect, both concepts similarly describe the shift from the hydroxylamine pathway to the AOB denitrification pathway. Considering FNA in Model G also indirectly enables the pH influence to be described.

The choice between these two concepts will depend on simulation objectives and calibration experience. Regarding the last extended model of Peng *et al.* (2016) which also includes the inorganic carbon effect (Model F), the ‘indirect coupling’ approach is able to reveal some metabolic relations between N<sub>2</sub>O production and the cell’s anabolism. This mathematical framework constitutes an ideal approach for investigating intracellular and metabolic mechanisms. In comparison, the direct coupling approach is simpler and easily understandable for practitioners as it is based on the conventional ASM approach. Another advantage of Model G is that it considers NO as an external state variable (not an intracellular compound like Model E) which makes it possible to use such data for model calibration (Pocquet *et al.*, 2016).

Finally, actual experience shows that both concepts enable good predictions. Work is now recommended with data from full-scale systems in which the mixed liquor complexity and the combination with other biochemical reactions could reveal stronger differences between these two models.

### 7.3.4 Key kinetic and stoichiometric parameters for calibration

The calibration approach for N<sub>2</sub>O models is based on two successive steps. The first step consists of adjusting the ‘conventional’ parameters (i.e., growth rate, decay rate, substrate removal rate and the

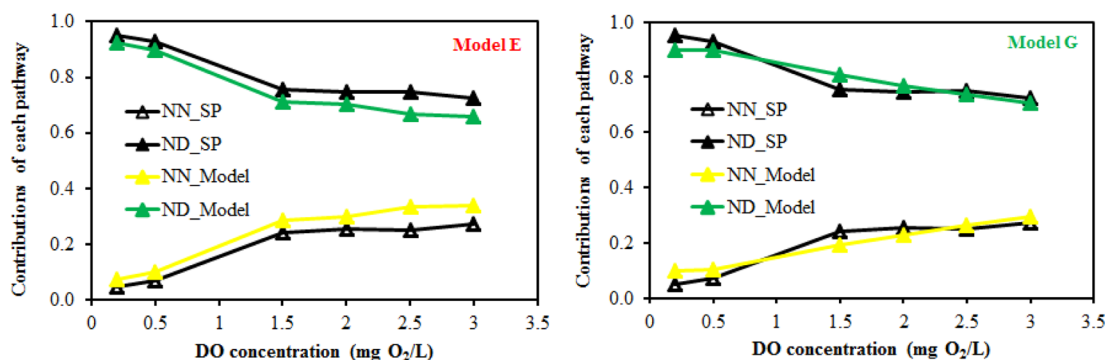


**Figure 7.7** Effect of dissolved oxygen on contribution of the two AOB pathways (left: Model E, right: Model G) SP: data from site-preference measurements (Lang *et al.*, 2017).

affinity constant) to obtain a good prediction of the main substances dynamics: ammonium, nitrite, nitrate, oxygen. In a second step, the specific parameters influencing  $N_2O$  emissions are calibrated. A final iteration should be performed if the prediction of the main substances is slightly affected by this second calibration step.

Typical values of the model parameters can be found in literature (Ni and Yuan, 2015). Different sets of parameter values obtained after calibration on different sets of data are provided by Spérandio *et al.* (2016) and Lang *et al.* (2017) for the single-pathway AOB models and the two-pathway AOB models, respectively. Continued testing against more experimental data would delineate a range/pattern in parameter values. It should be noted that these parameters were estimated under different conditions of temperature, sludge retention time and feeding composition, and therefore correction factors must be adjusted by, for example, Arrhenius equations (Snip *et al.*, 2014). Furthermore, the parameter values estimated during batch experiments may not be adequate for continuous processes and may not be compatible with the values of other parameters (Ni *et al.*, 2013a; Snip *et al.*, 2014; Spérandio *et al.*, 2016).

Regarding the ASM-ICE of the heterotrophic denitrifiers (Model OHO-B in Table S2), information on both the carbon oxidation reaction kinetics and the nitrogen reduction kinetics is required for its calibration and application (Table 7.2). Due to the lack of understanding of the electron competition process in most of the previous studies, the respective reaction kinetics of the carbon oxidation and nitrogen reduction processes were not well established. For instance, the maximum carbon source oxidation rate ( $r_{COD,max}$ ), which is the key parameter to restrict the overall model predictions of the carbon oxidation (electron supply) rate, is not available in literature and thus needs to be measured or estimated (Pan *et al.*, 2015). Similar to the two-pathway models of AOB, the relative ratios between electron affinity constants ( $K_{Mred,1}$ ,  $K_{Mred,2}$ ,  $K_{Mred,3}$ , and  $K_{Mred,4}$ ) rather than their absolute values are important for the reaction rate. Therefore, increased efforts are needed to provide more information on these key parameters of the ASM-ICE model for its further implementation (Table 7.2).

For the six single-pathway AOB models (Models A–D in Table S3), the model parameters were obtained after significant calibration efforts, and thus some of the parameters showed wide variation (more than 100%) among case studies during model evaluations (Ni *et al.*, 2011, 2013a; Spérandio *et al.*, 2016). Among them, the half saturation constant for nitrite or FNA ( $K_{NO_2,AOB}$  or  $K_{HNO_2,AOB}$  for Models A, A1, B, B1) and the reduction factor for  $N_2O$  production ( $\eta_{AOB}$ , for all six single-pathway models) were most variable and very influential on  $N_2O$  emissions (Spérandio *et al.*, 2016). Regarding the models based on the AOB denitrification pathway (e.g., Models A, A1, B and B1), the large variation of these two key parameters was related to the range of nitrite (or FNA) concentrations observed in each system (Spérandio *et al.*, 2016), likely due to the adaptation of enzymatic activity (NirK). Regarding the models based on the  $NH_2OH$  oxidation pathway (e.g., Models C and D) the large variation of  $\eta_{AOB}$  might be dependent on the possible NO accumulation in each system. High NO accumulation would lead to a low value for  $\eta_{AOB}$  (Spérandio *et al.*, 2016). Thus, calibration will be required for the application of the single-pathway models regarding these key parameters (Table 7.2).

For the electron balance-based two-pathway AOB models (Models E and F in Table S4), the affinity constants with respect to electrons (e.g.,  $K_{Mred,3}$  and  $K_{Mred,4}$ ) are unique to the two-pathway models and the key parameters governing the  $N_2O$  production via the two pathways. The values represent the affinity of the corresponding reduction reaction to electrons, with lower values indicating a higher affinity and thus a higher ability to compete for electrons. For example, the estimated  $K_{Mred,3}$  has a value that is about one magnitude smaller than  $K_{Mred,4}$  (Ni *et al.*, 2014), indicating that  $O_2$  reduction has a higher ability to compete for electrons than the main electron acceptor during  $NH_2OH$  oxidation. Ni *et al.* (2014) revealed that the absolute value of  $C_{tot}$  is not critical for model calibration and predictions, and it is the ratios between parameters  $K_{Mox}$ ,  $K_{Mred,1}$ ,  $K_{Mred,2}$ ,  $K_{Mred,3}$ , and  $K_{Mred,4}$  and parameter  $C_{tot}$  that affect the model output. Therefore, attention should be paid to these ratios for the calibration and application of the two-pathway models (see Table 7.2).

For the two-pathway model G, the reduction factor for both AOB denitrification and hydroxylamine pathway ( $\eta_{\text{AOB\_ND}}$ ,  $\eta_{\text{AOB\_NN}}$ ) are the two major influential parameters which control the maximal specific N<sub>2</sub>O production rates of each pathway (Lang *et al.*, 2017). The affinity constant for FNA also has to be calibrated from one culture to another, especially when working at very different nitrite concentrations. The hydroxylamine pathway contribution is also sensitive to the affinity constant for nitric oxide as determined by NO measurements (Pocquet *et al.*, 2016). In parallel, the AOB denitrification contribution is influenced by the inhibition constant for oxygen which is a key parameter for predicting the effect of lowering aeration on N<sub>2</sub>O emissions (Lang *et al.*, 2017).

Model H was calibrated following a global sensitivity analysis and an information-based parameter selection procedure (Domingo-Félez and Smets, 2020b; Domingo-Félez *et al.*, 2017). First, parameters associated with heterotrophic denitrification were fitted. Then, parameters associated with aerobic nitrite and ammonia oxidation were sequentially fitted to DO consumption profiles by isolating individual processes, followed by N<sub>2</sub>O production profiles. In the AOB-enriched biomass the reduction factors for the NN pathway and the N<sub>2</sub>O-production process were estimated together with the HNO<sub>2</sub> and NH<sub>2</sub>OH affinity constants. In the activated sludge mixed liquor biomass three reduction factors were estimated: NO-producing NN and ND pathways, and N<sub>2</sub>O production processes. The pH-dependency of AOB-driven N<sub>2</sub>O production and heterotrophic N<sub>2</sub>O consumption was also described (Domingo-Félez and Smets, 2020b; Su *et al.*, 2019a). The uncertainty associated with parameter estimation results was propagated to validate the model response, and is recommended to be included with best-fit simulations.

### 7.3.5 Application of N<sub>2</sub>O models in biofilm systems

The previous sections provide a basis for modelling the formation and consumption of N<sub>2</sub>O by AOB and heterotrophic denitrifying bacteria. In this section, we discuss how these kinetics are applied to biofilm processes. Biofilm treatment processes, such as the moving bed biofilm reactor (MBBR), integrated fixed-film activated sludge (IFAS), biological aerated filters (BAF), denitrifying filters, and granular sludge, are becoming increasingly popular for wastewater treatment. Due to substrate gradients and microbial stratification, the behaviour of biofilms is typically different from suspended growth processes, and this may be especially true for N<sub>2</sub>O production and emissions (Law *et al.*, 2012; Schreiber *et al.*, 2009; Sutka *et al.*, 2006). These systems appear to have among the highest N<sub>2</sub>O emission rates (e.g., Bollon *et al.*, 2016).

A schematic of a biofilm, with diffusion of substrates and products, is shown in Figure 7.8. In conventional biofilms, both the electron donor and acceptor substrates diffuse from the bulk liquid into the biofilm. Substrates penetrate into the biofilm by diffusion and are consumed within the biofilm by microbially catalysed reactions. Substrates diffusing into the biofilm from the bulk liquid side first pass the liquid diffusion (or boundary) layer. The liquid diffusion layer adds diffusive resistance to substrate transport into the biofilm, decreasing the substrate concentration at the biofilm surface with respect to the bulk liquid.

When modelling N<sub>2</sub>O emissions from biofilms, the underlying rate expressions are the same as those described for the suspended growth processes. However, diffusion and microbial stratification within the biofilm can change the observed behaviour. For example, suspended growth bacteria in an aerobic zone of a treatment process are unlikely to have appreciable denitrification. However, biofilms in aerobic zones of a treatment process may have anoxic zones in their interior. This can allow heterotrophic denitrification, including formation and consumption of N<sub>2</sub>O and AOB denitrification.

Sharp gradients of O<sub>2</sub> and other substrates within a biofilm, combined with different microbial species in close proximity, allow the diffusion of intermediates to different redox environments or zones with different microbial metabolisms. For example, NH<sub>2</sub>OH can be produced by AOB in the outer, aerobic zones of a biofilm, and consumed in inner, anoxic zones where it leads to peaks in N<sub>2</sub>O formation due to AOB denitrification. Nitrite oxidizing bacteria (NOB) can enhance this effect by increasing the O<sub>2</sub> gradients within the biofilm (Sabba *et al.* submitted).

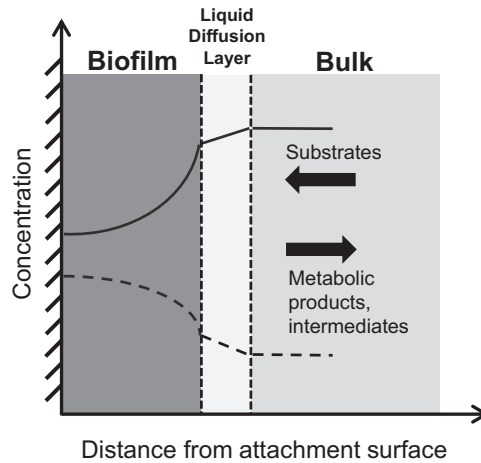


**Figure 7.8** Schematic of a biofilm with substrate penetration and metabolic products/intermediates formation.

The importance of intermediate diffusion is illustrated in [Figure 7.9](#), which shows  $\text{N}_2\text{O}$  emissions from a pilot-scale granular sludge reactor for side-stream nitrification ([Pijuan \*et al.\*, 2014](#)). When modelled with very limited  $\text{NH}_2\text{OH}$  diffusion (1% of the actual value), the model could not capture the actual  $\text{N}_2\text{O}$  emissions ([Figure 7.9](#)). However, when  $\text{NH}_2\text{OH}$  diffusion was included in the model, the model provided an excellent fit to the data ([Sabba \*et al.\*, 2015](#)).

Another example of interactions within a biofilm is the scavenging of  $\text{N}_2\text{O}$  formed in the outer zone of a biofilm, for example by AOB, by heterotrophic denitrifiers in the deeper, anoxic zones of the biofilm. This can lead to lower net  $\text{N}_2\text{O}$  emissions, although the complexity of biofilms makes this highly dependent on the specific reactor conditions.

Biofilm processes can be more challenging to calibrate than suspended growth processes. Information is needed about the biofilm thickness, density, substrate diffusivities, and microbial community structure. In most cases, a one-dimensional model can capture biofilm behaviour. Special care should be taken when analysing putative suspended-growth processes that may actually display biofilm behaviour. This may be true for processes with large flocs. It also may be true for bench- or pilot-scale systems, as reactor wall area is more significant, relative to reactor volume. This can lead to a greater impact of biofilms growing on walls than in a full-scale system.

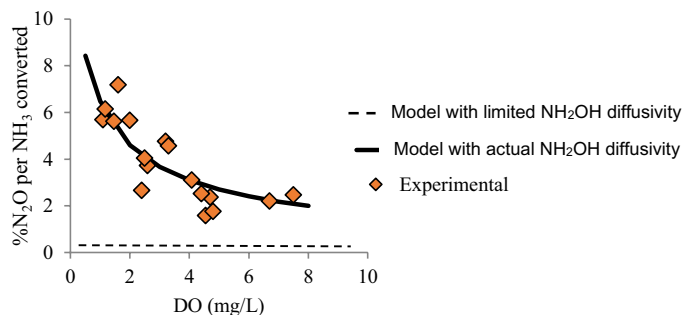


**Figure 7.9** Comparison between measured  $\% \text{N}_2\text{O}$  from  $\text{NH}_3$  converted and model-calculated values in steady-state conditions ([Sabba \*et al.\*, 2015](#)).

Recently the two pathway AOB model (G) and the multiple step denitrification model (OHO-A) were combined for describing N<sub>2</sub>O emissions from a nitrifying biofilter and denitrifying biofilter (Fiat *et al.*, 2019; Zhu *et al.*, 2019) as well as a granular sludge system (Lang *et al.*, 2019). Biofilm structure was described by a one-dimensional model. For a granular sludge partial nitrification anammox (PNA) system, the model was successfully calibrated to experimental data by adjusting the affinity constant for hydroxylamine mainly (Lang *et al.*, 2019). The effect of varying nitrite concentration and air flow rate was correctly predicted. Simulation demonstrated that a part of the N<sub>2</sub>O produced by AOB was consumed by heterotrophic denitrification in the biofilm, and N<sub>2</sub>O emission was highly influenced by the level of NOB repression. This work clarified the behaviour of N<sub>2</sub>O emission under very low oxygen concentration, indicating that nitrifier denitrification was the major contributing pathway.

Regarding the biofilters systems, the N<sub>2</sub>O models (A and G) were used in successive reactors to describe longitudinal heterogeneity in the biofilter. The simulations were compared to data monitored on full scale installations (results are described in the next paragraph).

In summary, biofilm processes are significantly more complex than suspended growth processes, and modelling can be a critical tool to understand the mechanisms and predict the N<sub>2</sub>O formation and emissions.

### 7.3.6 Application of N<sub>2</sub>O models in full-scale WWTPs

Mathematical modelling of N<sub>2</sub>O emissions from full-scale WWTPs was first conducted successfully by using ASM-type models that combine one of the single-pathway models of AOB with ASMN of heterotrophic denitrifiers (Ni *et al.*, 2013b). Ni *et al.* (2013b) applied a model based on the NH<sub>2</sub>OH pathway model of AOB (Model D, Table 7.1) and ASMN (Model OHO-A, Table 7.1) to describe the N<sub>2</sub>O emissions from full-scale WWTPs. The model described well the dynamic ammonium, nitrite, nitrate, DO and N<sub>2</sub>O data collected from both an open oxidation ditch (OD) system with surface aerators and a sequencing batch reactor (SBR) system with bubbling aeration. Ni *et al.* (2013b) also performed additional evaluations on the other three single-pathway N<sub>2</sub>O models of AOB (Model A, Model B and Model C in Table 7.1) to evaluate the experimentally observed N<sub>2</sub>O data from the two full-scale WWTPs. The results indicated that Model A could not predict the N<sub>2</sub>O data from either WWTP (Ni *et al.*, 2013b; Spérandio *et al.*, 2016). Models B and C, on the contrary, obtained very similar good fits between the model-predicted and experimentally observed N<sub>2</sub>O data (Ni *et al.*, 2013b, Spérandio *et al.*, 2016).

Dynamic simulations were also confronted to the data collected on the UCT (University Cape Town configuration) process of the Eindhoven plant by using ASM-type models that combine one of the single-pathway models of AOB with ASMN of heterotrophic denitrifiers (Guo and Vanrolleghem, 2014; Spérandio *et al.*, 2016). Model A1 + Model OHO-A, Model B1 + Model OHO-A and Model D + Model OHO-A were all implemented for this plant and calibrated using data collected in a 1-month measurement campaign. The conclusion was that all these models could be calibrated to the same level of fit (Spérandio *et al.*, 2016). They had similar performance and could follow the dynamic variations in the measured N<sub>2</sub>O data (see Figure 7.10). In addition, the results showed that there was less N<sub>2</sub>O emission under wet-weather conditions compared to dry-weather conditions and all three models showed better simulation performance under dry-weather conditions than wet-weather conditions (Spérandio *et al.*, 2016).

Mathematical modelling of N<sub>2</sub>O emissions from full-scale WWTPs was then conducted successfully by using electron balance-based models that integrate the two-pathway model of AOB and the ASMN of heterotrophic denitrifiers (Ni *et al.*, 2015). Ni *et al.* (2015) applied an integrated model incorporating the electron balance-based two-pathway model of AOB (Model E, Table 7.1) and the ASMN of heterotrophic denitrifiers (Model OHO-A, Table 7.1) to describe N<sub>2</sub>O emissions from a step-feed full-scale WWTP. The model described well all dynamic ammonium, nitrite, nitrate, DO and N<sub>2</sub>O emission data. Modelling results revealed that the AOB denitrification rate decreased and the NH<sub>2</sub>OH oxidation rate increased along the path of both steps, with the second step of the full-scale

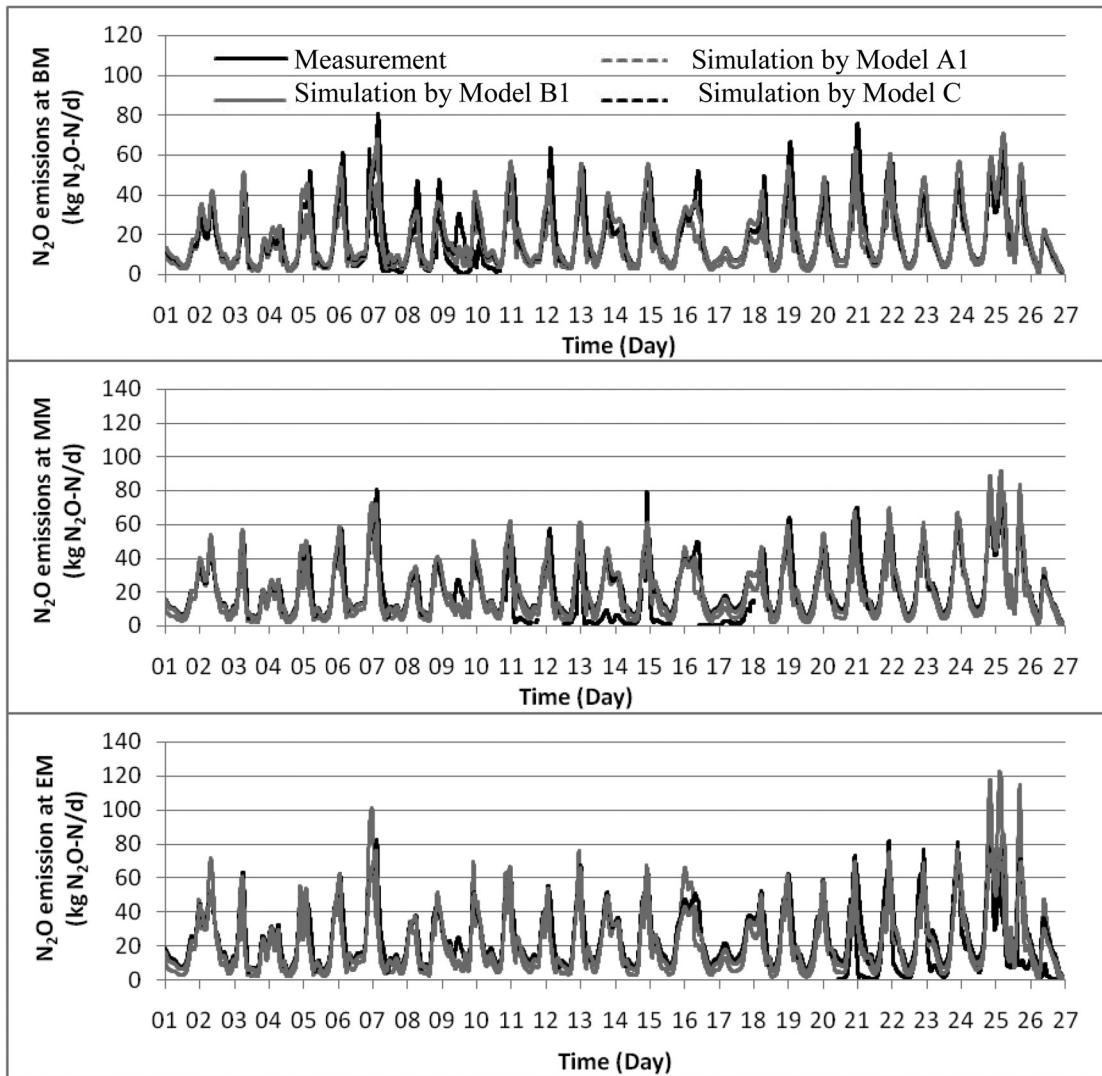


**Figure 7.10** Model evaluation results for  $\text{N}_2\text{O}$  emissions using the measurement results at the beginning (BM) (upper panel), the middle (MM) (middle panel) and the end section (EM) (bottom panel) of the summer aeration package on the UCT process at the Eindhoven treatment plant by using ASM-type models that combine one of the single-pathway models of AOB (Models A1, B1 and C) with the ASMN (Model OHO-A) of heterotrophic denitrifiers (Spérandio *et al.*, 2016).

WWTP having much higher  $\text{N}_2\text{O}$  emission than the first step. The integrated  $\text{N}_2\text{O}$  model captured all these trends regarding the shifting/distribution between the different  $\text{N}_2\text{O}$  pathways observed in this full-scale WWTP (see Figure 7.11). A potential strategy to mitigate  $\text{N}_2\text{O}$  emission from this plant was also evaluated using the model. The overall  $\text{N}_2\text{O}$  emission from the step-feed WWTP would be largely mitigated if 30% of the returned activated sludge was returned to the second step with the remaining 70% returning to the first step.

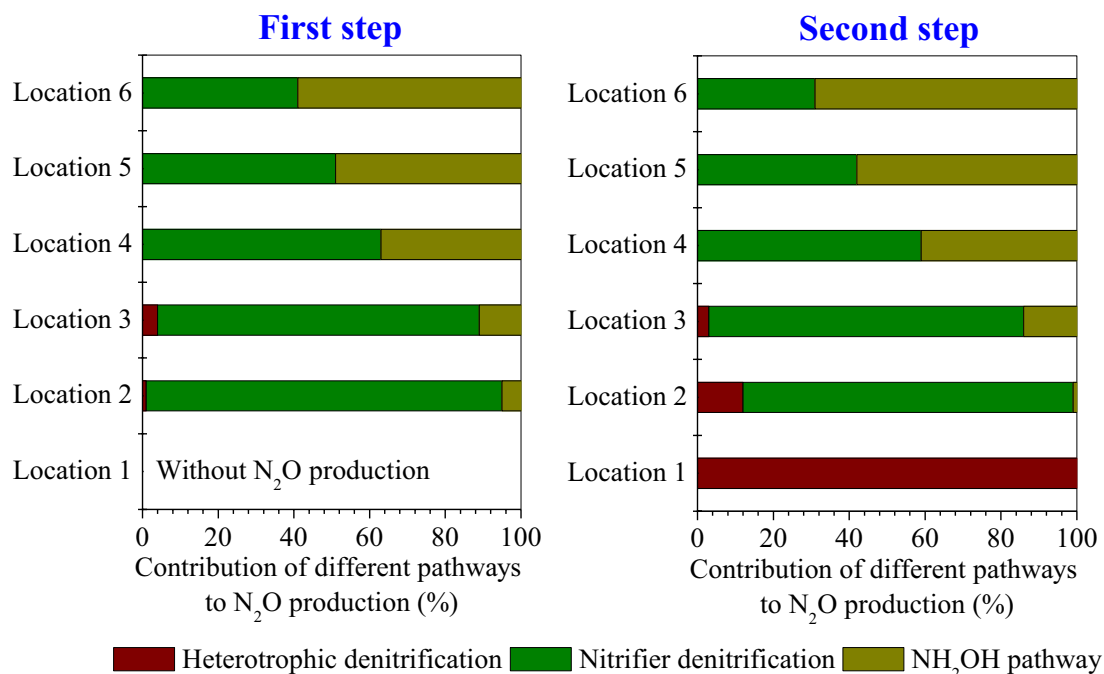


**Figure 7.11** Model predicted percentage contributions from the three N<sub>2</sub>O pathways to total N<sub>2</sub>O productions at six different locations of the first step (left panel) and the second step (right panel) in the step-feed full-scale WWTP, that is, the nitrifier denitrification pathway, the NH<sub>2</sub>OH pathway and the heterotrophic denitrification pathway (Ni *et al.*, 2015).

More recently, the electron balance-based model (Model F) has been successfully applied to guide a full-scale N<sub>2</sub>O mitigation study (Duan *et al.*, 2020). Full-scale treatment plants have inevitably more complexities than laboratory reactor operations (Ahn *et al.*, 2010a, b; de Haas and Hartley, 2004; Foley *et al.*, 2010; Inventory of U.S. Greenhouse Gas Emissions and Sinks: 1990–2010 (2012); IPCC, 2007; Ye *et al.*, 2014). It was inconclusive whether the model predictions can be reliably applied to guide full-scale mitigations. In this recent work, Model F was calibrated and validated against full-scale results, before being applied to predict the N<sub>2</sub>O emissions and nutrient removal performances with different N<sub>2</sub>O mitigation measures. The close agreement between the measured emission factor (EF) ( $0.58 \pm 0.06\%$ ) after the implementation of the proposed mitigation strategy, and the EF predicted by the mathematical model (0.55%), showed that the N<sub>2</sub>O mathematical model is indeed a useful tool to evaluate N<sub>2</sub>O mitigation strategies at full-scale. The model can be a powerful tool for the prediction of N<sub>2</sub>O emissions from full-scale WWTPs and development of effective mitigation strategies, although it may require more efforts on model calibration.

Regarding biofilm systems, only a few studies are currently available at full scale. In the work of Fiat *et al.* (2019) and Zhu *et al.* (2019) tertiary nitrifying and denitrifying biofilters were modelled including the main N<sub>2</sub>O biological pathways. Simulations were confronted to full-scale data from Seine Aval, the largest wastewater resource recovery facility in Europe. Zhu *et al.* (2019) obtained a satisfying prediction of the emission factor which was higher in the winter period (5.9%) than the value obtained in the summer period (2.9%), in accordance with experimental observations. Fiat *et al.* (2019) demonstrated that the model should include a mass balance on the gaseous phase in each reactor compartment of the BAF in order to correctly describe the N<sub>2</sub>O gas-liquid partition

and  $N_2O$  emissions. Preliminary modifications of the model structure were made to include the gas phase as a compartment of the model, which significantly affected the prediction of nitrification. In particular, considering gas hold-up influenced the prediction of the hydraulic retention time, and thus nitrification performances. Finally, the value of the volumetric oxygen transfer coefficient was adjusted to successfully predict both nitrification and  $N_2O$  emissions.

It should be noted that there are still only a limited number of studies presented in literature regarding the real application of  $N_2O$  models at full-scale WWTPs although many full-scale measurement campaigns have been performed in different places during recent years. More full-scale applications of the models using these full-scale  $N_2O$  data are still needed for the models to be developed into a useful tool for practical applications. In addition, the requirement for good fundamental knowledge on  $N_2O$  emission by the modeller/engineer might also hinder the  $N_2O$  model applications due to the complicated procedure for model selection and calibration, which consequently limit the development of effective mitigation strategies. Hopefully this chapter will facilitate the selection of suitable  $N_2O$  models, the estimation of site-specific  $N_2O$  emissions and the development of mitigation strategies for wastewater treatment plants taking into account the specific design and operational conditions of the plant.

## 7.4 CONCLUSIONS AND PERSPECTIVES

In this chapter, the existing  $N_2O$  models available in literature based on the three major  $N_2O$  production pathways were reviewed and compared to illuminate their structural differences, their capabilities and inabilities in describing experimental data, and their potential range of applications. The key conclusions are:

- Our understanding of fundamental mechanisms related to  $N_2O$  production and consumption has strongly progressed in recent decades, leading to the development of  $N_2O$  models with different mathematical structures but relatively similar metabolic pathways.

- For AOB, the two-pathway models have the potential to describe most of the  $N_2O$  data. The combined effect of DO and nitrite is described well by these models, either based on the direct or indirect coupling approach. In comparison, the single-pathway models can be used under several particular conditions depending on the concentrations of oxygen and nitrite which determine the dominating pathway. Despite calibration works still being necessary, recent studies have demonstrated good prediction capabilities for both lab-scale and full-scale observations. The uncertainties around parameters and their propagation on prediction should be considered appropriately.

- For heterotrophic denitrifiers, the ASM<sub>N</sub>-type model was the most used model for predicting the overall nitrogen and COD removal performance in the case where there is only low accumulation of intermediates, whereas new alternatives have been proposed recently and should be considered in the future. In a heterotrophic denitrifier biofilm, the potential for  $N_2O$  accumulation together with its consumption in the inner biofilm should be taken into account. The ASM-ICE type model has the potential to describe all  $N_2O$  data, but requires more information on reaction kinetics. Full-scale data sets still need to be properly consolidated by adding highly different reactor set-ups, measurement methods, culture history, documentation, and/or interpretations, which would limit the failure of model predictions. Numerous full-scale data sets are starting to be available for suspended growth systems. However, very few studies have identified emissions from biofilm systems.

- Future efforts should be devoted to comparing the multiple pathway models to data from real WWTPs to observe the key differences and to enhance their practical applications. Ideally, more information on pathway contributions should be collected in such systems (by means of isotope techniques, or  $NO:N_2O$  ratio variations).

- Although suspended growth models seem to capture  $N_2O$  emissions efficiently, biofilm mechanisms of  $N_2O$  production need further investigation. Only a few experiences with mathematical modelling of  $N_2O$  emission from biofilm systems have been reported and this should also be conducted using more monitoring data from such systems.

Mathematical modelling of N<sub>2</sub>O production has reached a maturity that facilitates the estimation of site-specific N<sub>2</sub>O emissions and the development of mitigation strategies. Although existing models still have limitations, their application will undoubtedly increase in the near future. Their confrontation to full-scale data should improve the robustness of the parameters and would certainly suggest further model improvement. For instance the coupling of an N<sub>2</sub>O model with more detailed description of hydrodynamics and heterogeneities is probably a future need. Integration of N<sub>2</sub>O models with the models describing other sections of the WWTPs into a plant-wide model could be a powerful tool for future optimization works.

## ACKNOWLEDGEMENTS

Research on N<sub>2</sub>O emissions at INSA-TBI was supported by the French National Research Agency (ANR) through the research project N<sub>2</sub>OTrack. Longqi Lang was supported by a scholarship granted by the China Scholarship Council. Zhiguo Yuan is a recipient of the ARC Laureate Fellowship (FL170100086). Research on N<sub>2</sub>O dynamics at DTU has been supported by the Danish Agency for Science, Technology and Innovation through the Research Project LaGas (12-132633), the Danish Council for Independent Research through Project N<sub>2</sub>Oman (17H01893) and the Danish Ministry of Environment and Food through the MUDP project HEPWAT. Research at Notre Dame on N<sub>2</sub>O emissions from biofilm processes has been supported by NSF project CBET0954918 and WERF project U2R10. Additional support was provided by a Bayer Corporation Fellowship to F.S.

## REFERENCES

- Ahn J. H., Kim S., Park H., Rahm B., Pagilla K. and Chandran K. (2010a). N<sub>2</sub>O emissions from activated sludge processes, 2008–2009: results of a national monitoring survey in the United States. *Environmental Science & Technology*, **44**, 4505–4511, <https://doi.org/10.1021/es903845y>
- Ahn J. H., Kim S., Park H., Katehis D., Pagilla K. and Chandran K. (2010b). Spatial and temporal variability in atmospheric nitrous oxide generation and emission from full-scale biological nitrogen removal and non-BNR processes. *Water Environment Research*, **82**, 2362–2372, <https://doi.org/10.2175/106143010X12681059116897>
- Almeida J. S., Reis M. A. M. and Carrondo M. J. T. (1997). A unifying kinetic model of denitrification. *Journal of Theoretical Biology*, **186**(2), 241–249, <https://doi.org/10.1006/jtbi.1996.0352>
- Arp D. J. and Stein L. Y. (2003). Metabolism of inorganic N compounds by ammonia-oxidizing bacteria. *Critical Reviews in Biochemistry and Molecular Biology*, **38**, 471–495, <https://doi.org/10.1080/10409230390267446>
- Arp D. J., Chain P. S. G. and Klotz M. G. (2007). The impact of genome analyses on our understanding of ammonia-oxidizing bacteria. *Annual Review of Microbiology*, **61**, 503–528, <https://doi.org/10.1146/annurev.micro.61.080706.093449>
- Bollon J., Filali A., Fayolle Y., Guerin S., Rocher V. and Gillot S. (2016). N<sub>2</sub>O emissions from full-scale nitrifying biofilters. *Water Research*, **102**, 41–51, <https://doi.org/10.1016/j.watres.2016.05.091>
- Castro-Barros C. M., Daelman M. R. J., Mampaey K. E., van Loosdrecht M. C. M. and Volcke E. I. P. (2015). Effect of aeration regime on N<sub>2</sub>O emission from partial nitrification-anammox in a full-scale granular sludge reactor. *Water Research*, **68**, 793–803, <https://doi.org/10.1016/j.watres.2014.10.056>
- Chandran K., Stein L. Y., Klotz M. G. and van Loosdrecht M. C. M. (2011). Nitrous oxide production by lithotrophic ammonia-oxidizing bacteria and implications for engineered nitrogen-removal systems. *Biochemical Society Transactions*, **39**, 1832–1837, <https://doi.org/10.1042/BST20110717>
- Corominas L., Flores-Alsina X., Snip L. and Vanrolleghem P. A. (2012). Comparison of different modelling approaches to better understand and minimize greenhouse gas emissions from wastewater treatment plants. *Biotechnology and Bioengineering*, **109**, 2854–2863, <https://doi.org/10.1002/bit.24544>
- CH2MHill. (2008). Discussion paper for a wastewater treatment plant sector greenhouse gas emissions reporting protocol, Final report prepared for California Wastewater Climate Change Group, Oakland, California.
- de Haas D. and Hartley K. J. (2004). Greenhouse gas emissions from BNR plant – do we have the right focus? Proceedings: Sewage Management – Risk Assessment and Triple Bottom Line. Queensland Environmental Protection Agency, April 2004, Cairns, pp. 5–7.

- Domingo-Félez C. and Smets B. F. (2016). A consilience model to describe N<sub>2</sub>O production during biological N removal. *Environmental Science: Water Research & Technology*, **2**, 923–930, <https://doi.org/10.1039/C6EW00179C>
- Domingo-Félez C. and Smets B. F. (2020a). Modelling denitrification as an electric circuit accurately captures electron competition between individual reductive steps: the activated sludge model–electron competition model. *Environmental Science & Technology*, **54**(12), 7330–7338, <https://doi.org/10.1021/acs.est.0c01095>
- Domingo-Félez C. and Smets B. F. (2020b). Modelling N<sub>2</sub>O dynamics of activated sludge biomass: Uncertainty analysis and pathway contributions. *Chemical Engineering Journal*, **379**, 122311, <https://doi.org/10.1016/j.cej.2019.122311>
- Domingo-Félez C., Calderó-Pascual M., Sin G., Plósz B. G. and Smets B. F. (2017). Calibration of the comprehensive NDHA-N<sub>2</sub>O dynamics model for nitrifier-enriched biomass using targeted respirometric assays. *Water Research*, **126**, 29–39, <https://doi.org/10.1016/j.watres.2017.09.013>
- Duan H., van den Akker B., Thwaites B. J., Peng L., Herman C., Pan Y., Ni B. J., Watt S., Yuan Z. and Ye L. (2020). Mitigating nitrous oxide emissions at a full-scale wastewater treatment plant. *Water Research*, 116196, <https://doi.org/10.1016/j.watres.2020.116196>
- Fiat J., Filali A., Fayolle Y., Bernier J., Rocher V., Spérandio M. and Gillot S. (2019). Considering the plug-flow behavior of the gas phase in nitrifying BAF models significantly improves the prediction of N<sub>2</sub>O emissions. *Water Research*, **156**, 337–346, <https://doi.org/10.1016/j.watres.2019.03.047>
- Foley J., de Haas D., Yuan Z. and Lant P. (2010). Nitrous oxide generation in full-scale biological nutrient removal wastewater treatment plants. *Water Research*, **44**, 831–844, <https://doi.org/10.1016/j.watres.2009.10.033>
- Guo L. and Vanrolleghem P. A. (2014). Calibration and validation of an activated sludge model for greenhouse gases No. 1 (ASMG1) – prediction of temperature dependent N<sub>2</sub>O emission dynamics. *Bioprocess and Biosystems Engineering*, **37**, 151–163, <https://doi.org/10.1007/s00449-013-0978-3>
- Harper Jr, W. F., Takeuchi Y., Riya S., Hosomi M. and Terada A. (2015). Novel abiotic reactions increase nitrous oxide production during partial nitrification: modelling and experiments. *Chemical Engineering Journal*, **281**, 1017–1023, <https://doi.org/10.1016/j.cej.2015.06.109>
- Harris E., Joss A., Emmenegger L., Kipf M., Wolf B., Mohn J. and Wunderlin P. (2015). Isotopic evidence for nitrous oxide production pathways in a partial nitrification-anammox reactor. *Water Research*, **83**, 258–270, <https://doi.org/10.1016/j.watres.2015.06.040>
- Hiatt W. C. and Grady Jr, C. P. L. (2008). An updated process model for carbon oxidation, nitrification, and denitrification. *Water Environment Research*, **80**, 2145–2156, <https://doi.org/10.2175/106143008X304776>
- Hooper A. B., Vannelli T., Bergmann D. J., and Arciero D. M. (1997). Enzymology of the oxidation of ammonia to nitrite by bacteria. *Antonie Van Leeuwenhoek*, **71**, 59–67, <https://doi.org/10.1023/A:1000133919203>
- Inventory of U.S. Greenhouse Gas Emissions and Sinks: 1990–2010. (2012). EPA 430-R-12-001. U. S. Environmental Protection Agency, Washington, DC.
- IPCC. (2007). Climate Change 2007: The Physical Science Basis. In: Contribution of Working Group I to the Fourth Assessment Report of the Intergovernmental Panel on Climate Change, S. Solomon, D. Qin, M. Manning, Z. Chen, M. Marquis, K. B. Averyt, M. Tignor and H. L. Miller (eds.), Cambridge University Press, Cambridge, United Kingdom and New York, NY, USA.
- Kampschreur M. J., Picioreanu C., Tan N., Kleerebezem R., Jetten M. S. M. and van Loosdrecht M. C. M. (2007). Unraveling the source of nitric oxide emission during nitrification. *Water Environment Research*, **79**, 2499–2509, <https://doi.org/10.2175/106143007X220815>
- Kampschreur M. J., Temmink H., Kleerebezem R., Jetten M. S. M. and van Loosdrecht M. C. M. (2009). Nitrous oxide emission during wastewater treatment. *Water Research*, **43**, 4093–4103, <https://doi.org/10.1016/j.watres.2009.03.001>
- Kim S. W., Miyahara M., Fushinobu S., Wakagi T. and Shoun H. (2010). Nitrous oxide emission from nitrifying activated sludge dependent on denitrification by ammonia-oxidizing bacteria. *Bioresource Technology*, **101**, 3958–3963, <https://doi.org/10.1016/j.biortech.2010.01.030>
- Lang L., Pocquet M., Ni B.J., Yuan Z. and Spérandio M. (2017). Comparison of different 2-pathway models for describing the combined effect of DO and nitrite on the nitrous oxide production by ammonia-oxidizing bacteria. *Water Science and Technology*, **75**(3), 491–500, <https://doi.org/10.2166/wst.2016.389>
- Lang L., Piveteau S., Azimi S., Rocher V. and Spérandio M. (2019). Modelling N<sub>2</sub>O emission from PNA process under oxygen limitation: model calibration and prospects. Proceeding of Watermatex 2019 Conference, 1–4 September 2019, Copenhagen, Denmark.

- Law Y., Ni B. J., Lant P. and Yuan Z. (2012). Nitrous oxide (N<sub>2</sub>O) production by an enriched culture of ammonia oxidising bacteria depends on its ammonia oxidation rate. *Water Research*, **46**, 3409–3419, <https://doi.org/10.1016/j.watres.2012.03.043>
- Law Y., Lant P. A. and Yuan Z. (2013). The confounding effect of nitrite on N<sub>2</sub>O production by an enriched ammonia-oxidising culture. *Environmental Science & Technology*, **47**, 7186–7194, <https://doi.org/10.1021/es4009689>
- Lu H. and Chandran K. (2010). Factors promoting emissions of nitrous oxide and nitric oxide from denitrifying sequencing batch reactors operated with methanol and ethanol as electron donors. *Biotechnology and Bioengineering*, **106**, 390–398, <https://doi.org/10.1002/bit.22704>
- Mannina G., Ekama G., Caniani D., Cosenza A., Esposito G., Gori R., Garrido-Baserba M., Rosso D. and Olsson G. (2016). Greenhouse gases from wastewater treatment – a review of modelling tools. *Science of the Total Environment*, **551–552**, 254–270, <https://doi.org/10.1016/j.scitotenv.2016.01.163>
- Mampaey K. E., Beuckels B., Kampschreur M. J., Kleerebezem R., Van Loosdrecht M. C. M. and Volcke E. I. P. (2013). Modelling nitrous and nitric oxide emissions by autotrophic ammonia-oxidizing bacteria. *Environmental Technology*, **34**, 1555–1566, <https://doi.org/10.1080/09593330.2012.758666>
- Mampaey K., Spérandio M., van Loosdrecht M. C. M. and Volcke E. I. P. (2019). Dynamic simulation of N<sub>2</sub>O emissions from a full-scale partial nitrification reactor. *Biochemical Engineering Journal*, **152**, 107356, <https://doi.org/10.1016/j.bej.2019.107356>
- Ni B. J. and Yuan Z. (2015). Recent advances in mathematical modelling of nitrous oxides emissions from wastewater treatment processes. *Water Research*, **87**, 336–346, <https://doi.org/10.1016/j.watres.2015.09.049>
- Ni B. J., Rusalleda M., Pellicer-Nacher C. and Smets B. F. (2011). Modelling nitrous oxide production during biological nitrogen removal via nitrification and denitrification: extensions to the general ASM models. *Environmental Science & Technology*, **45**, 7768–7776, <https://doi.org/10.1021/es201489n>
- Ni B. J., Yuan Z., Chandran K., Vanrolleghem P. A. and Murthy S. (2013a). Evaluating four mathematical models for nitrous oxide production by autotrophic ammonia-oxidizing bacteria. *Biotechnology and Bioengineering*, **110**, 153–163, <https://doi.org/10.1002/bit.24620>
- Ni B. J., Ye L., Law Y., Byers C. and Yuan Z. (2013b). Mathematical modelling of nitrous oxide (N<sub>2</sub>O) emissions from full-scale wastewater treatment plants. *Environmental Science & Technology*, **47**, 7795–7803, <https://doi.org/10.1021/es4005398>
- Ni B. J., Peng L., Law Y., Guo J. and Yuan Z. (2014). Modelling of nitrous oxide production by autotrophic ammonia-oxidizing bacteria with multiple production pathways. *Environmental Science & Technology*, **48**, 3916–392, <https://doi.org/10.1021/es405592h>
- Ni B. J., Pan Y., van den Akker B., Ye L. and Yuan Z. (2015). Full-scale modelling explaining large spatial variations of nitrous oxide fluxes in a step-feed plug-flow wastewater treatment reactor. *Environmental Science & Technology*, **49**, 9176–9184, <https://doi.org/10.1021/acs.est.5b02038>
- Okabe S., Oshiki M., Takahashi Y. and Satoh H. (2011). N<sub>2</sub>O emission from a partial nitrification–anammox process and identification of a key biological process of N<sub>2</sub>O emission from anammox granules. *Water Research*, **45**, 6461–6470, <https://doi.org/10.1016/j.watres.2011.09.040>
- Pan Y., Ye L., Ni B. J. and Yuan Z. (2012). Effect of pH on N<sub>2</sub>O reduction and accumulation during denitrification by methanol-utilizing denitrifiers. *Water Research*, **46**(15), 4832–4840, <https://doi.org/10.1016/j.watres.2012.06.003>
- Pan Y., Ni B. J., Bond P. L., Ye L. and Yuan Z. (2013a). Electron competition among nitrogen oxides reduction during methanol-utilizing denitrification in wastewater treatment. *Water Research*, **47**(10), 3273–3281, <https://doi.org/10.1016/j.watres.2013.02.054>
- Pan Y., Ni B. J. and Yuan Z. (2013b). Modelling electron competition among nitrogen oxides reduction and N<sub>2</sub>O accumulation in denitrification. *Environmental Science & Technology*, **47**, 11083–11091, <https://doi.org/10.1021/es402348n>
- Pan Y., Ni B. J., Lu H., Chandran K., Richardson D. and Yuan Z. (2015). Evaluating two concepts for the modelling of intermediates accumulation during biological denitrification in wastewater treatment. *Water Research*, **71**, 21–31, <https://doi.org/10.1016/j.watres.2014.12.029>
- Peng L., Ni B. J., Erler D., Ye L. and Yuan Z. (2014). The effect of dissolved oxygen on N<sub>2</sub>O production by ammonia-oxidizing bacteria in an enriched nitrifying sludge. *Water Research*, **66**, 12–21, <https://doi.org/10.1016/j.watres.2014.08.009>
- Peng L., Ni B. J., Law Y. and Yuan Z. (2015a). Modelling of N<sub>2</sub>O production by ammonia oxidizing bacteria: integration of catabolism and anabolism. The 9th IWA Symposium on Systems Analysis and Integrated Assessment (Watermatex 2015), 14–17 June, Gold Coast, Australia.

- Peng L., Ni B. J., Ye L. and Yuan Z. (2015b). Selection of mathematical models for  $N_2O$  production by ammonia oxidizing bacteria under varying dissolved oxygen and nitrite concentrations. *Chemical Engineering Journal*, **281**, 661–668, <https://doi.org/10.1016/j.cej.2015.07.015>
- Peng L., Ni B. J., Law Y. and Yuan Z. (2016). Modeling  $N_2O$  production by ammonia oxidizing bacteria at varying inorganic carbon concentrations by coupling the catabolic and anabolic processes. *Chemical Engineering Science*, **144**, 386–394.
- Perez-Garcia O., Villas-Boas S. G., Swift S., Chandran K. and Singhal N. (2014). Clarifying the regulation of  $NO/N_2O$  production in *Nitrosomonas europaea* during anoxic-oxic transition via flux balance analysis of a metabolic network model. *Water Research*, **60**, 267–277, <https://doi.org/10.1016/j.watres.2014.04.049>
- Pijuan M., Tora J., Rodriguez-Caballero A., Cesar E., Carrera J. and Perez J. (2014). Effect of process parameters and operational mode on nitrous oxide emissions from a nitrification reactor treating reject wastewater. *Water Research*, **49**, 23–33, <https://doi.org/10.1016/j.watres.2013.11.009>
- Pocquet M., Queinnec I. and Spérandio M. (2013). Adaptation and identification of models for nitrous oxide ( $N_2O$ ) production by autotrophic nitrite reduction. Proceedings 11th IWA Conference on Instrumentation, Control and Automation (ICA2013), 18–20 September, Narbonne, France.
- Pocquet M., Wu Z., Queinnec I. and Spérandio M. (2016). A two pathway model for  $N_2O$  emissions by ammonium oxidizing bacteria supported by the  $NO/N_2O$  variation. *Water Research*, **88**, 948–959.
- Poughon L., Dussap C. G. and Gros J. B. (2000). Energy model and metabolic flux analysis for autotrophic nitrifiers. *Biotechnology and Bioengineering*, **72**, 416–433, [https://doi.org/10.1002/1097-0290\(20000220\)72:4<416::AID-BIT1004>3.0.CO;2-D](https://doi.org/10.1002/1097-0290(20000220)72:4<416::AID-BIT1004>3.0.CO;2-D)
- Sabba F., Picioreanu C., Pérez J. and Nerenberg R. (2015). Hydroxylamine diffusion can enhance  $N_2O$  emissions in nitrifying biofilms: a modelling study. *Environmental Science & Technology*, **49**, 1486–1494, <https://doi.org/10.1021/es5046919>
- Schreiber F., Loeffler B., Polerecky L., Kuypers M. M. M. and de Beer D. (2009). Mechanisms of transient nitric oxide and nitrous oxide production in a complex biofilm. *The ISME Journal*, **3**, 1301–1313, <https://doi.org/10.1038/ismej.2009.55>
- Snip L. J. P., Boiocchi R., Flores-Alsina X., Jeppsson U. and Gernaey K. V. (2014). Challenges encountered when expanding activated sludge models: a case study based on  $N_2O$  production. *Water Science and Technology*, **70**(7), 1251–1260, <https://doi.org/10.2166/wst.2014.347>
- Spérandio M., Pocquet M., Guo L., Vanrolleghem P., Ni B. J. and Yuan Z. (2016). Evaluation of different nitrous oxide production models with four continuous long-term wastewater treatment process data series. *Bioprocess and Biosystems Engineering*, **39**, 493–510, <https://doi.org/10.1007/s00449-015-1532-2>
- Stein L. Y. (2011a). Surveying  $N_2O$ -producing pathways in bacteria. *Methods in Enzymology*, **486**, 131–152, <https://doi.org/10.1016/B978-0-12-381294-0.00006-7>
- Stein L. Y. (2011b). Heterotrophic nitrification and nitrifier denitrification. In: Nitrification, B. B. Ward, D. J. Arp and M. G. Klotz (eds.), American Society for Microbiology Press, Washington DC, pp. 95–114.
- Su Q., Domingo-Félez C., Zhang Z., Blum J. M., Jensen M. M. and Smets B. F. (2019a). The effect of pH on  $N_2O$  production in intermittently-fed nitrification reactors. *Water Research*, **156**, 223–231, <https://doi.org/10.1016/j.watres.2019.03.015>
- Su Q., Domingo-Félez C., Jensen M. M. and Smets B. F. (2019b) Abiotic nitrous oxide ( $N_2O$ ) production is strongly pH dependent, but contributes little to overall  $N_2O$  emissions in biological nitrogen removal systems. *Environmental Science & Technology*, **53**(7), 3508–3516, <https://doi.org/10.1021/acs.est.8b06193>
- Sutka R., Ostrom N., Ostrom P., Breznak J., Gandhi H., Pitt A. and Li F. (2006). Distinguishing nitrous oxide production from nitrification and denitrification on the basis of isotopomer abundances. *Applied Environmental Microbiology*, **72**(1), 638–644, <https://doi.org/10.1128/AEM.72.1.638-644.2006>
- Talleg G., Garnier J., Billen G. and Gossais M. (2006). Nitrous oxide emissions from secondary activated sludge in nitrifying conditions of urban wastewater treatment plants: effect of oxygenation level. *Water Research*, **40**, 2972–2980, <https://doi.org/10.1016/j.watres.2006.05.037>
- Vasilaki V., Conca V., Frison N., Eusebi A. L., Fatone F. and Katsou, E. (2020). A knowledge discovery framework to predict the  $N_2O$  emissions in the wastewater sector. *Water Research*, **178**, 115799, <https://doi.org/10.1016/j.watres.2020.115799>
- von Schulthess R. and Gujer W. (1996). Release of nitrous oxide ( $N_2O$ ) from denitrifying activated sludge: Verification and application of a mathematical model. *Water Research*, **30**(3), 521–530, [https://doi.org/10.1016/0043-1354\(95\)00204-9](https://doi.org/10.1016/0043-1354(95)00204-9)

- Wunderlin P., Mohn J., Joss A., Emmenegger L. and Siegrist H. (2012). Mechanisms of N<sub>2</sub>O production in biological wastewater treatment under nitrifying and denitrifying conditions. *Water Research*, **46**, 1027–1037, <https://doi.org/10.1016/j.watres.2011.11.080>
- Wunderlin P., Lehmann M. F., Siegrist H., Tuzson B., Joss A., Emmenegger L. and Mohn J. (2013). Isotope signatures of N<sub>2</sub>O in a mixed microbial population system: constraints on N<sub>2</sub>O producing pathways in wastewater treatment. *Environmental Science & Technology*, **47**, 1339–1348, <https://doi.org/10.1021/es402971p>
- Yang Q., Liu X., Peng C., Wang S., Sun H. and Peng Y. (2009). N<sub>2</sub>O Production during nitrogen removal via nitrite from domestic wastewater: main sources and control method. *Environmental Science & Technology*, **43**, 9400–9406, <https://doi.org/10.1021/es9019113>
- Ye L., Ni B.-J., Law Y., Byers C. and Yuan Z. (2014). A novel methodology to quantify nitrous oxide emissions from full-scale wastewater treatment systems with surface aerators. *Water Research*, **48**, 257–268, <https://doi.org/10.1016/j.watres.2013.09.037>
- Yu R., Kampschreur M. J., van Loosdrecht M. C. M. and Chandran K. (2010). Mechanisms and specific directionality of autotrophic nitrous oxide and nitric oxide generation during transient anoxia. *Environmental Science & Technology*, **44**, 1313–1319, <https://doi.org/10.1021/es902794a>
- Zaborowska E., Lu X. and Makinia J. (2019). Strategies for mitigating nitrous oxide production and decreasing the carbon footprint of a full-scale combined nitrogen and phosphorus removal activated sludge system. *Water Research*, **162**, 53–63, <https://doi.org/10.1016/j.watres.2019.06.057>
- Zhu J., Bernier J., Patry B., Azimi S., Pauss A., Rocher V. and Vanrolleghem P. A. (2019). Comprehensive modelling of full-scale nitrifying and post-denitrifying biofilters. Proceedings WEF Nutrient Removal and Recovery Symposium 2019 – 21st Century Vision, 23–25 July 2019, Minneapolis, MN, USA.

## NOMENCLATURE

ADP	Adenosine diphosphate
AMO	Ammonia monooxygenase
AOB	Ammonia-oxidizing bacteria
ASM	Activated sludge model
ASM-EC	Activated sludge model – electron competition
ASM-ICE	Activated sludge model with indirect coupling of electrons
ASMN	Activated sludge model for nitrogen
ATP	Adenosine triphosphate
COD	Chemical oxygen demand
DO	Dissolved oxygen
EF	Emission factor
FA	Free ammonia
FNA	Free nitrous acid
HAO	Hydroxylamine oxidoreductase
IC	Inorganic carbon
Mox	Electron carriers in oxidized form
Mred	Electron carriers in reduced form
N <sub>2</sub> OR	N <sub>2</sub> O reductase
Nar	Nitrate reductase
ND	Nitrifiers denitrification

Nir	Nitrite/nitric oxide oxidoreductase
NirK	Nitrite reductase
NN	Hydroxylamine pathway
NOB	Nitrite oxidizing bacteria
NOR	NO reductase
OHO	Ordinary heterotrophic organisms
SP	Site-preference
sNOR	Haem-copper nitric oxide reductase
WWTP	Wastewater treatment plant

Table S1 in the supplementary information (SI) lists the definitions of the all the state variables used in the models described in this chapter. Please see doi: [10.2166/9781789060461\\_S1](https://doi.org/10.2166/9781789060461_S1)